


 Cite this: *RSC Adv.*, 2026, 16, 2062

## Recent advances in cassane diterpenoids: structural diversity and biological activities

 Sabrin R. M. Ibrahim,<sup>ab</sup> Hagar M. Mohamed,<sup>cd</sup> Samar S. A. Murshid,<sup>e</sup> Asma Ahmad Nashawi<sup>f</sup> and Gamal A. Mohamed<sup>e</sup>

Cassane diterpenoids are naturally occurring compounds, characterized mainly by molecular skeletons of three fused cyclohexane rings. They are predominantly isolated from the genus *Caesalpinia* (*Fabaceae*). Cassane diterpenoids possess various pharmacological activities, including anti-inflammatory, antibacterial, cytotoxic, antiparasitic, antidiabetic, and neuroprotective effects. This work provides an update on the newly reported cassane diterpenoids from 2019 to 2025. In this work, cassane diterpenoids are categorized according to their carbon skeletons into usual tricyclic cassanes, tricyclic cassane with butanolide, cassane furanoditerpenoids, norcassanes, cassane ester amines, cassane amides, and penta-spiro cassanes. Their reported biological activities, together with biosynthetic pathways, isolation and purification, and structure–activity relationships, are discussed. A total of 238 compounds were discussed, and 55 references were listed. The reported findings expand the knowledge of chemical features and biological potential of cassane diterpenoids and support their further investigation as promising leads for drug discovery.

Received 18th September 2025

Accepted 26th December 2025

DOI: 10.1039/d5ra07088k

[rsc.li/rsc-advances](https://rsc.li/rsc-advances)

### 1. Introduction

The shared challenges that people face worldwide include attaining zero hunger, ending poverty, improving nutritional status, enhancing people's health, promoting sustainable agriculture, delivering affordable health care services, and limiting climate change. The UN General Assembly passed a resolution titled "Transforming our world: the 2030 agenda for sustainable development," that included 17 SDGs (Sustainable Development Goals). Providing a sustainable global health care system by 2030 is among these SDGs, and global efforts have been directed towards finding new and innovative solutions for achieving this goal. Medicinal plants are among the most important sources of medicine, and millions of people rely on herbal medicine for their treatments and cures. Additionally, their constituents have long been known to play an essential

role in the development and discovery of therapeutic agents because of their remarkable structural diversity and wide range of bioactivities. Terpenes are the largest, most common class of natural secondary metabolites, comprising over 30 000 members found in all organisms, particularly the higher plants.<sup>1</sup> Among them, diterpenoids consisting of four isoprene units, are distinguished by their wide range of pharmacological properties and structural features. Cassane diterpenoids are characterized by a *trans-trans*-fused tricyclic (6/6/6) carbon skeleton consisting of three fused cyclohexane rings (A, B, and C) with a C-13 ethyl and C-14 methyl substituent, and a typical *trans-trans* ring junction between rings A/B and B/C. The configuration at the chiral centers is generally 5*S*/8*S*/9*S*/10*R*, which is essential for maintaining the rigidity of the fused ring system and influences biological activities. Some cassane diterpenoids feature a tetracyclic core with a fused  $\alpha,\beta$ -butenolide (lactone-type),  $\alpha,\beta$ -unsaturated  $\gamma$ -lactam, or furan ring.<sup>1,2</sup> Some derivatives with diverse nitrogen or oxygen bridges and opened A ring have been reported; cassane alkaloids are a structurally unique category of diterpenoid alkaloids.<sup>3</sup> Additionally, tetracyclic or pentacyclic cassane-type alkaloids possessing a C-19/C-20 N-bridge, as well as hexacyclic and nonacyclic cassane derivatives with substitutions such as alkyl, hydroxyl, and acetyl groups, have been isolated.<sup>4–6</sup> Cassane diterpenoids are mainly reported from various genera of the *Fabaceae* family, particularly the genus *Caesalpinia*. These compounds possess diverse bioactivities, including bactericidal, antimalarial, immunomodulatory, antibacterial, anti-hyperglycemic, anti-inflammatory, antitubercular, antioxidant, anthelmintic,

<sup>a</sup>Preparatory Year Program, Department of Chemistry, Batterjee Medical College, Jeddah 21442, Saudi Arabia. E-mail: [sabrin.ibrahim@bmc.edu](mailto:sabrin.ibrahim@bmc.edu); Tel: +966-581183034

<sup>b</sup>Department of Pharmacognosy, Faculty of Pharmacy, Assiut University, Assiut 71526, Egypt

<sup>c</sup>Department of Medical Laboratory Analysis, College of Medical & Health Sciences, Liwa University, Abu Dhabi 41009, United Arab of Emirates. E-mail: [Hagar.aly@lc.ac.ae](mailto:Hagar.aly@lc.ac.ae)

<sup>d</sup>Department of Applied Medical Chemistry, Medical Research Institute, Alexandria University, Alexandria, Egypt. E-mail: [Hagar-aly@hotmail.com](mailto:Hagar-aly@hotmail.com)

<sup>e</sup>Department of Natural Products and Alternative Medicine, Faculty of Pharmacy, King Abdulaziz University, Jeddah 21589, Saudi Arabia. E-mail: [samurshid@kau.edu.sa](mailto:samurshid@kau.edu.sa); [gahusseini@kau.edu.sa](mailto:gahusseini@kau.edu.sa)

<sup>f</sup>Department of Pharmaceutical Chemistry, Faculty of Pharmacy, King Abdulaziz University, Jeddah 21589, Saudi Arabia. E-mail: [anashawi@kau.edu.sa](mailto:anashawi@kau.edu.sa)



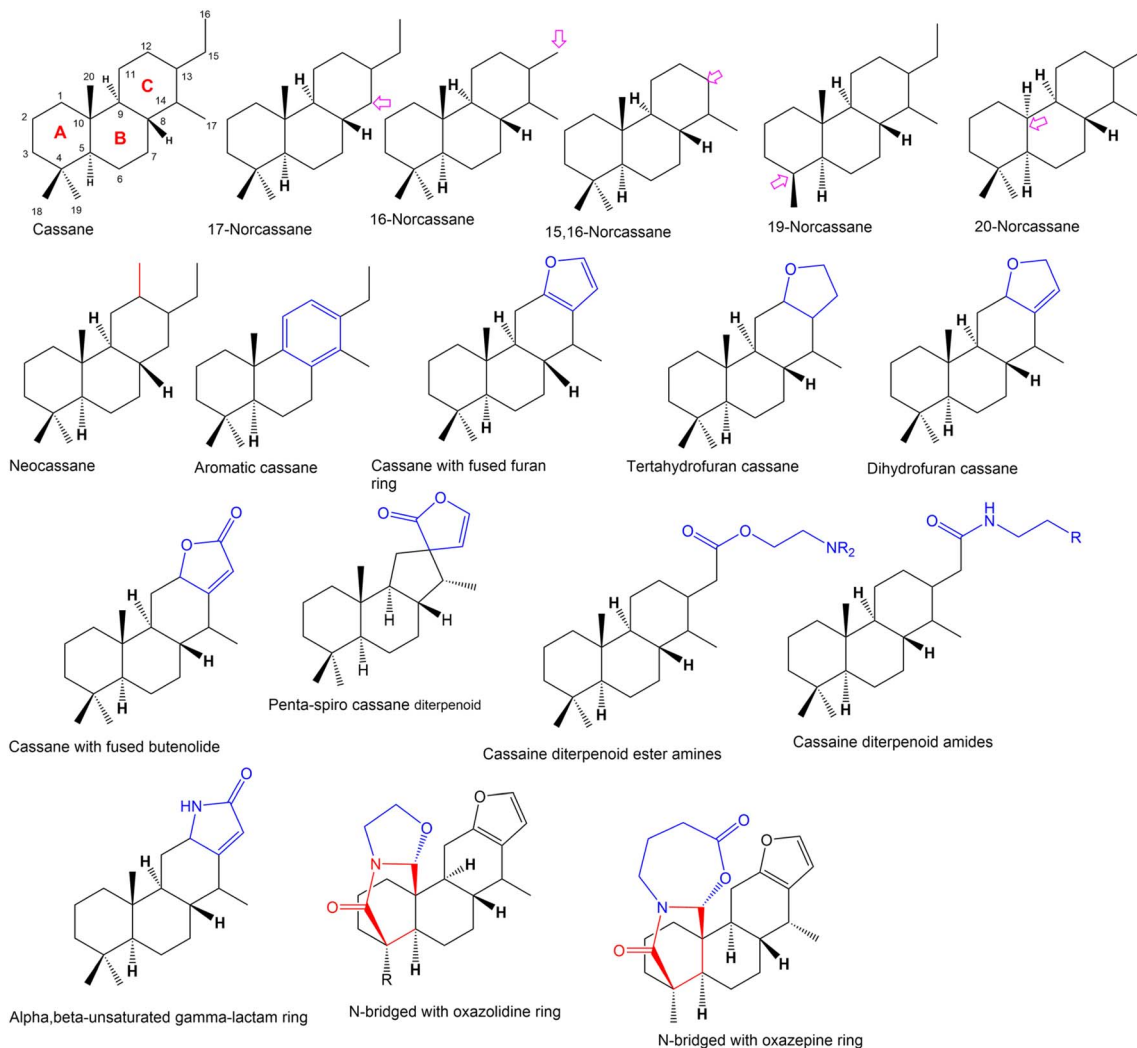


Fig. 1 Different classes of cassane diterpenoids.

antiproliferative, antiviral, antiparasitic, and neuroprotective effects.

Previously published works by Jing *et al.* and Maurya *et al.* comprehensively reviewed naturally occurring cassane derivatives, including their biosynthetic origins, classifications, and pharmacological characteristics.<sup>2,7</sup> Since 2019, many new cassane diterpenoids with diverse skeletons and biological activities have been reported. The current review provides an update on the reported new derivatives between 2019 and 2025. These compounds were categorized according to their carbon skeleton into different classes, including usual tricyclic cassane diterpenoids, neocassane diterpenoids, cassane diterpenoids with butanolide moiety, cassane furanoditerpenoids, norcassane diterpenoids, cassane diterpenoids ester amine, cassane diterpenoid amides, and penta-spiro cassane diterpenoids (Fig. 1). Additionally, their isolation, purification, biosynthesis, biological properties, and structure–activity relationships are discussed. The results presented in this study broaden the knowledge on chemical characteristics and biological advantages of cassane diterpenoids that encourage their further investigations as possible leads for drug discovery.

## 2. Literature search

A comprehensive literature search was done through various databases (ScienceDirect, PubMed, Google Scholar, and Scopus) and publishers' websites (Wiley, ACS, Bentham, Wiley, Taylor & Francis, Elsevier, and Springer) with special focus on the published articles from 2019 to 2025. The search was performed using the following keywords: “Cassane diterpenoids”, “*Caesalpinia*”, “Cassane diterpenoids + biological activity”, “Cassane diterpenoids + pharmacology”, “Cassane diterpenoids + biosynthesis”, “Cassane diterpenoids + isolation”. The articles that reported isolation, chemical structures, biosynthetic pathways, and biological effects of new cassane diterpenoids were included. Publications in non-peer-reviewed sources, irrelevant reports, or those fully written in non-English language were excluded. In total, 238 cassane diterpenoids were reviewed from the cited studies. A total of 55 references were analyzed to provide a comprehensive overview of their structural diversity, isolation, biosynthesis, and biological properties.



### 3. Isolation, purification, and characterization

For the separation of cassane diterpenoids, dried, powdered plant materials, including stem roots, leaves, aerial parts, fruits, roots, seeds, and root barks were extracted using various solvents such as 80% MeOH, 95% EtOH, dichloromethane/MeOH, 75% EtOH, and 85% EtOH. The extracts were liquid-liquid partitioned with PE/CHCl<sub>3</sub>/n-BuOH, PE/EtOAc/n-BuOH, CHCl<sub>3</sub>/BuOH, or PE/CHCl<sub>3</sub>/EtOAc. In most studies, extracts were further subjected to Diaion HP-20 open column chromatography (CC) (H<sub>2</sub>O/MeOH), SiO<sub>2</sub> CC (petroleum ether/acetone 30:1–0:1 or 40:1–0:1; CH<sub>2</sub>Cl<sub>2</sub>/CH<sub>3</sub>OH 100:0–1:1; CH<sub>2</sub>Cl<sub>2</sub>-acetone 100:0–1:1), flash diol CC (hexane/EtOAc and EtOAc/MeOH gradients), SiO<sub>2</sub> flash CC (CH<sub>2</sub>Cl<sub>2</sub>-MeOH 1:0 to 0:1), and polyamide CC using H<sub>2</sub>O, 30% EtOH, 60% EtOH, or 95% EtOH. Further separation was done using Sephadex LH-20 columns with MeOH (100%) and RP-18 CC with MeOH:H<sub>2</sub>O of different polarity. Resulting fractions were subjected to various chromatographic tools such as RP-C18 flash CC (MeCN-H<sub>2</sub>O gradients), polyamide columns, flash chromatography with CH<sub>2</sub>Cl<sub>2</sub>/MeOH (1–50%), Sephadex LH-20 (CHCl<sub>3</sub>-MeOH 1:1), SiO<sub>2</sub> CC using various eluent systems [PE-Me<sub>2</sub>CO; PE-EtOAc (20:1, 10:1–1:1, 7:1–1:1, or 20:1/15:1/7:1/4:1/3:1/2:1/1:1); CHCl<sub>3</sub>/Me<sub>2</sub>CO; acetone:hexane (3:7)], normal RP-18 CC (MeOH-H<sub>2</sub>O 75:25, 4:6–9:1), MPLC on MCI gel columns

(MeOH/H<sub>2</sub>O 40/60 to 100/0; Me<sub>2</sub>CO-H<sub>2</sub>O 7/3 to 1/0), or ODS columns were also used. For final purification, HPLC was utilized using gradients such as CH<sub>3</sub>CN/H<sub>2</sub>O (70:30, 85:15, 45:55, 70–90%, 50:50, 47:53; 95:5–0:100), MeOH/H<sub>2</sub>O (6:4; 75:25), Sephadex LH-20 (MeOH), or preparative TLC plates were also used (CH<sub>2</sub>Cl<sub>2</sub>-MeOH 100:1; CH<sub>2</sub>Cl<sub>2</sub>-acetone 50:1). For nitrogen-containing derivatives, acid-base extraction techniques were employed to isolate the alkaloidal fractions, using CH<sub>2</sub>Cl<sub>2</sub> and EtOAc. These alkaloids were further purified by HPLC using solvent systems such as 0.1% formic acid in H<sub>2</sub>O (A) and CAN (B) with a 5–100% B gradient, or CH<sub>3</sub>CN-H<sub>2</sub>O containing 0.1% formic acid (85:15 to 50:50).

In general, the reported findings demonstrated that cassane diterpenoids have considerable lipophilicity as oxygenated metabolites. In practice, the most effective extraction of dried plant material is accomplished through thorough extraction employing medium-to-high polarity solvents, mainly methanol or 70–95% aqueous ethanol, and, in a few cases, acetone. The seeds and seed kernels of *Caesalpinia* species usually are defatted with PE/hexane, followed by an extraction with 75–95% ethanol or methanol, after which the crude extract is suspended in water and partitioned into chloroform, dichloromethane, or ethyl acetate layers. On the other hand, the aerial parts, leaves, fruits, roots, and bark are typically extracted directly using methanol or high-concentration ethanol and handled similarly. Cassane diterpenoids are usually concentrated in medium-

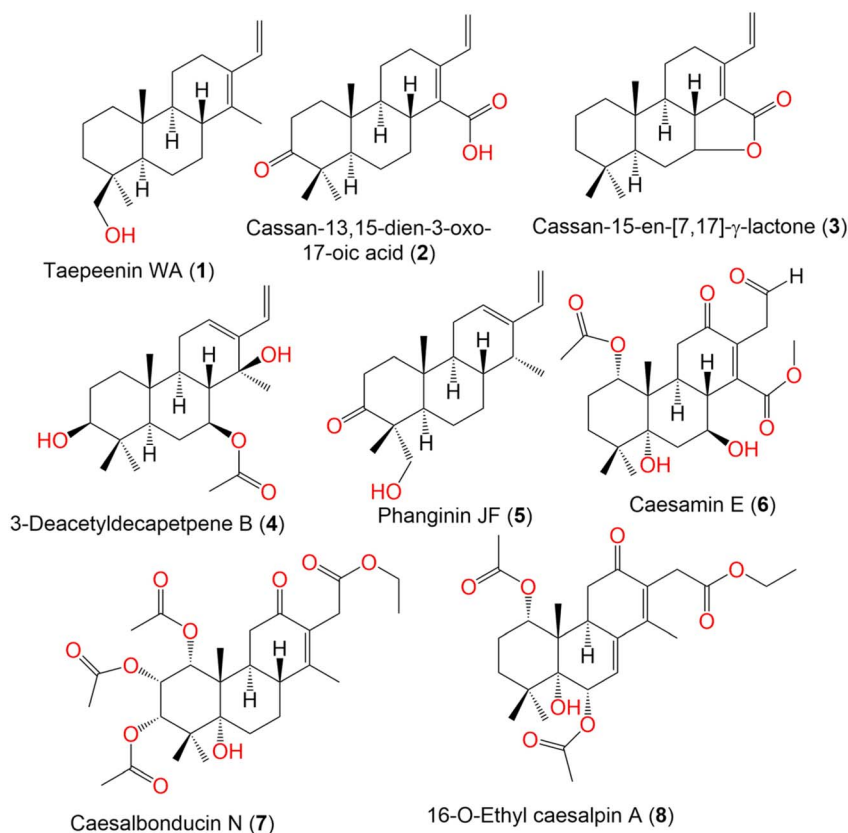


Fig. 2 Chemical structures of usual cassane diterpenoids (1–8).



polarity organic fractions across various species and plant parts, while the highly non-polar PE/hexane layers mainly extract lipids and waxes, and the highly aqueous phase retains polar components instead of cassanes.<sup>8–15</sup> This combination of hydroalcoholic extraction followed by CHCl<sub>3</sub>/CH<sub>2</sub>Cl<sub>2</sub>/EtOAc partition therefore seems to be the most suitable solvent system for cassane diterpenoids, as it matches their amphiphilic nature; where the tricyclic diterpene core requires non-polar organic solvent, while the polar substituents (hydroxyl, ester, lactone, glycosidic, or nitrogenous moieties) need polar solvent for efficient solubilization and chromatographic separation. Crude MeOH/EtOH extracts typically represent about 3–14% of the dry plant weight, while cassane-enriched CHCl<sub>3</sub>/CH<sub>2</sub>Cl<sub>2</sub>/EtOAc fractions account for about 0.5–3% of the original plant material, and individual cassane diterpenoids were obtained in milligram amounts, confirming them as minor secondary metabolites.<sup>12,16–20</sup> Within this context, several practical steps appear useful to modestly improve recovery: to remove unnecessary components and minimize losses during the following chromatographic steps, defatting with PE/hexane before hydroalcoholic extraction, applying thorough 75–95% EtOH or MeOH extraction (ultrasound, reflux, or successive maceration processes), carefully optimizing the CHCl<sub>3</sub>/CH<sub>2</sub>Cl<sub>2</sub>/EtOAc partition step, and introducing an initial enrichment step on polymeric adsorbent resins (*e.g.* Diaion HP-20, MCI gel) or medium-pressure RP-18 columns to concentrate medium-polarity cassane diterpenoids before detailed column chromatography.

Cassane diterpenoids' structures were established by IR and NMR spectroscopy, including <sup>1</sup>H, <sup>13</sup>C, COSY, ROESY, HSQC, and HMBC. Molecular weights were confirmed by HRESIMS and Q-TOF-MS. The configurations were assigned using optical rotation, NOESY, ROESY, coupling constant values, X-ray crystallography, quantum chemical calculations, and electronic circular dichroism (ECD).

## 4. Cassane diterpenoids and their bioactivities

### 4.1. Usual cassane diterpenoids

Konan *et al.* characterized **2**, **3**, and **21** from *Erythrophleum suaveolens* root bark CH<sub>2</sub>Cl<sub>2</sub> and EtOAc fractions.<sup>21</sup> Compounds **2** and **3** are similar to cassan-13,15-dien-17-oic acid, with C-3 ketone and a C-7-C17 ester groups, respectively, whereas **21** is related to cassamic acid with an additional alpha-6-OH group.<sup>21</sup> Compound **4** showed moderate to strong cytotoxic activity, being potent against MCF-7 (IC<sub>50</sub> 8.00 μM) and moderately active toward HEY and A549 cells (IC<sub>50</sub> 10.74 and 25.34 μM, respectively).<sup>22</sup> Structurally, compound **4** differs from related cassane derivatives by bearing a methyl group in place of the carboxylic acid (COOH) at C-17.<sup>22</sup> These structural modifications may contribute to the observed variation in cytotoxic potency. Huang *et al.* isolated compounds **8** and **9** from the seeds of *Caesalpinia minax* Hance<sup>12</sup> that are structurally similar to caesalpins A and B, respectively (Fig. 2).

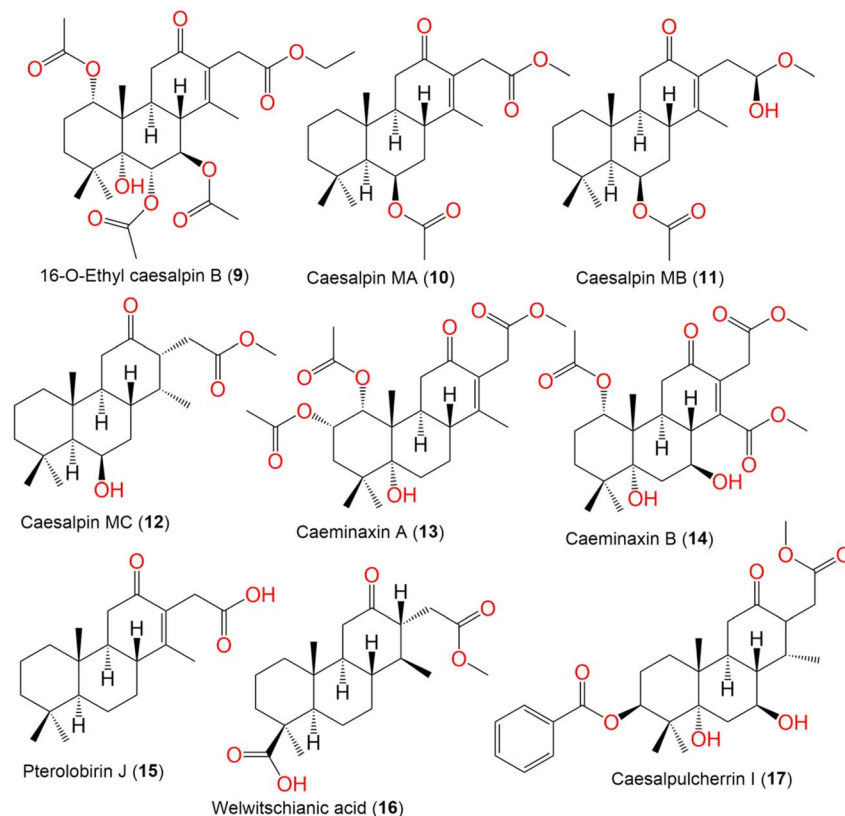


Fig. 3 Chemical structures of usual cassane diterpenoids (9–17).



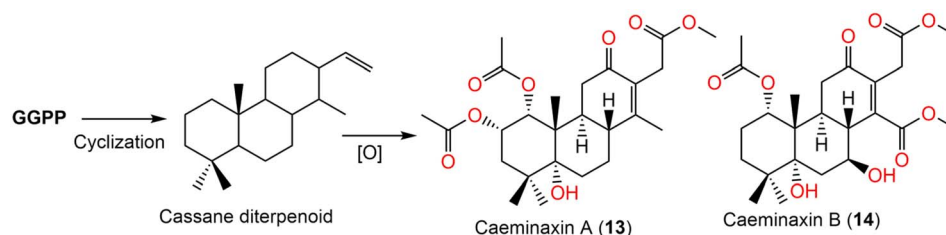
These two compounds have an ethoxy group instead of the methoxy group in caesalpins A and B and share the same 1*S*/5*R*/6*S*/7*R*/8*R*/9*S*/10*S* configuration (Fig. 3). They did not have lipid-lowering potential in oleic acid/palmitic acid-treated AML12 hepatocytes.<sup>12</sup> The tricyclic cassane diterpenoids: **10–12** were isolated from *Caesalpinia sinensis* seed kernels (Table S1).<sup>23</sup>

The configuration of **12** was assigned as 5*S*/6*R*/8*S*/9*S*/10*R*/13*R*/14*R* based on ECD and Xray analyses, while **10**, having an additional double bond at C13–C14 and an acetoxy group replacing 6-OH, possesses the same spatial arrangement at C8. The apparent 8*R*/8*S* difference results only from ligand priority conventions rather than a true configurational change. Compound **11** has CH<sub>2</sub>CHO substituent at C-16 instead of the carbonyl carbon and possesses 5*R*/6*R*/8*R*/9*S*/10*R*/16*R* configuration.<sup>23</sup> These compounds prohibited LPS-produced NO formation (inhibition rate 40.3–67.3%) in RAW 264.7 cells compared to dexamethasone (inhibition rate 51.2%), with **12**

was the most active (inhibition rate 67.3%; Conc. 10 μM) metabolite. It had potent NO inhibition capacity by reducing the iNOS activity in the Nitric Oxide Synthase Assay.<sup>23</sup>

Compounds **13** and **14** possess conjugated unsaturated carbonyl moiety and were proposed to be biosynthesized from GGPP *via* cyclization and successive oxidations (Scheme 1). These compounds demonstrated potent anti-inflammatory efficacy (IC<sub>50</sub>s 10.86 and 12.76 μM, respectively) than quercetin (IC<sub>50</sub> 13.28 μM) towards LPS-boosted NO production in the BV-2 microglial cells.<sup>24</sup> Compound **13** remarkably prohibited iNOS and COX-2 expressions induced by LPS in BV-2 microglial cells. It also demonstrated anti-inflammation capacity by inhibiting MAPK phosphorylation and NF-κB activation (Table S2).<sup>24</sup>

Bioassay-guided fractionation of the methanolic extract of *Caesalpinia welwitschiana* led to the isolation **16**, a tricyclic cassane with a C12 ketone, C-19 carboxyl, and C15



Scheme 1 Biosynthesis of **13** and **14**.<sup>24</sup> Adapted from ref. 24, with permission from Elsevier. © 2023 Elsevier. License no. 6178030849466.

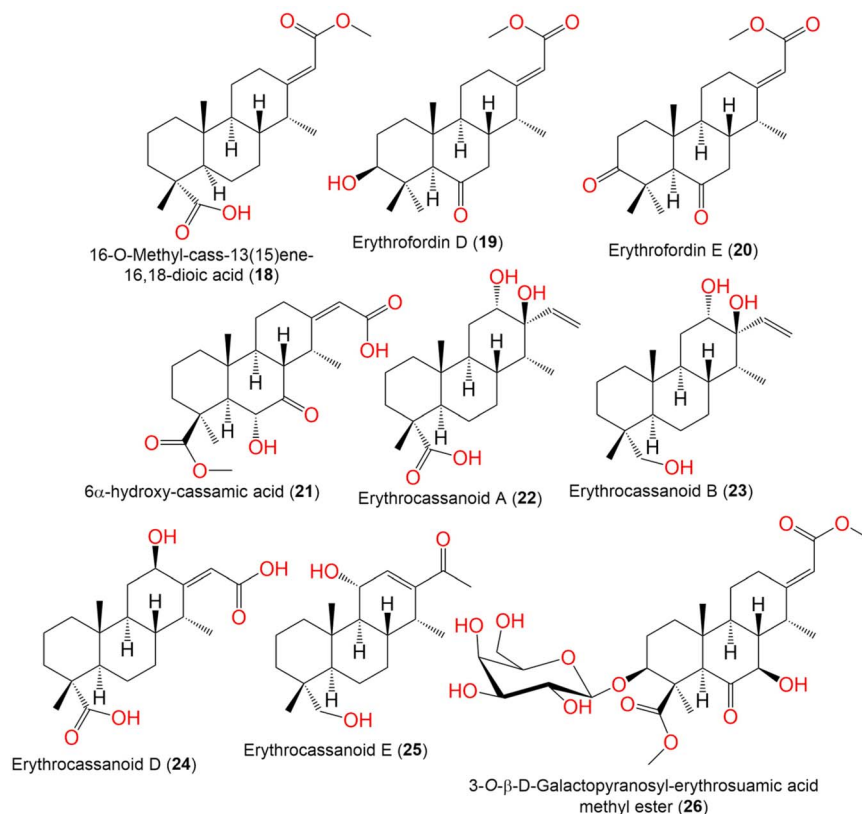


Fig. 4 Chemical structures of usual cassane diterpenoids (**18–26**).



carbomethoxy groups. It showed weak antifeedant and ovicidal capacity against *Tuta absoluta* (tomato pinworm).<sup>25</sup> Bitchi *et al.* separated a new cassane-type diterpene, **18**, from *Parkia bicolor* stem roots,<sup>26</sup> which is a C<sub>13</sub> esterified tricyclic cassane diterpenoid with a C-14 CH<sub>3</sub> group. Compound **18** was inactive at 100 μM concentration against K562 cells in the MTS assay, compared with doxorubicin (IC<sub>50</sub> 0.59 μM).<sup>26</sup>

Besides, compounds **19** and **20**, isolated from *Erythrophleum suaveolens*, feature a C-13 *exo-α,β*-unsaturated methyl ester, while **20** has a C-3 carbonyl group in instead of the 3-OH present in compound **19** (Fig. 4). These metabolites exhibited strong cytotoxic potential (GI<sub>50</sub>s 2.45 and 0.71 μM; TGIs 9.77 and 2.29 μM; LC<sub>50</sub>s 26.92 and 11.48 μM, respectively) in the NCI-60 cancer cell panel. Additionally, they (Conc. 0.03 μg mL<sup>-1</sup>) demonstrated significant cardiotoxicity in human cardiomyocytes derived from induced pluripotent stem cells.<sup>27</sup> Compounds **22–25** are undescribed cassane diterpenoids isolated from *Erythrophleum fordii* roots 95% EtOH extract by Li *et al.* Compounds **22**, **23**, **24**, and **25** feature olefinic double bond at C-15-C16, C-15-C13, and C-12-C-13, respectively.<sup>28</sup> These compounds were inactive against both coxsackie and influenza viruses.<sup>28</sup>

From *Erythrophleum suaveolens* seeds extract, **26** was further separated; it possesses a terminal methyl ester group and a 3-O-β-D-

galactopyranosyl. Compound **26** was inactive against A-549, MCF-7, and HCT-116 cell lines (IC<sub>50</sub> > 100 μM).<sup>11</sup> Compounds **27–32** separated from *Caesalpinia mimosoides* seeds, feature 18-COOCH<sub>3</sub> and different degree of oxidation at C-12, C-15, and C-16 (Fig. 5). These compounds were assessed for their inhibitory effects on TGF-β1-induced renal fibrosis in NRK-52E cells. It was noted that higher oxidation degree of the C ring at C-15,16 and the multiple OH groups boosted the antifibrotic activity (*e.g.*, **29**, **30**, **31**, and **32**).<sup>29</sup>

Additionally, **37** new tricyclic cassane diterpenes with an  $\alpha, \beta$ -unsaturated carbonyl moiety was identified from *Pterolobium macropterum* seeds.<sup>30</sup> It exhibited inhibition capacity (IC<sub>50</sub> 47.57 μM) versus LPS-simulated NO formation in BV-2 microglial cells.<sup>30</sup> Compound **38** is a diterpene with 3*S*/5*S*/8*R*/9*S*/10*R*/13*R*/14*R*/15*R* configuration and a rare 6''/6/6/3'' carbon skeleton.<sup>31</sup> Compound **38** exhibited powerful antibacterial potential towards *B. cereus* and *S. aureus* (MICs 6.25 and 3.13 μM, respectively) compared with gentamicin (3.13 and 3.13 μM, respectively). It induced bacterial cell death by increasing membrane permeability and suppressing growth.<sup>31</sup>

#### 4.2. Neocassane diterpenoids

The bioassay-guided fractionation of *Eragrostis plana* roots hexane, CH<sub>2</sub>Cl<sub>2</sub>/MeOH (1 : 1) and water (H<sub>2</sub>O) extracts (Conc

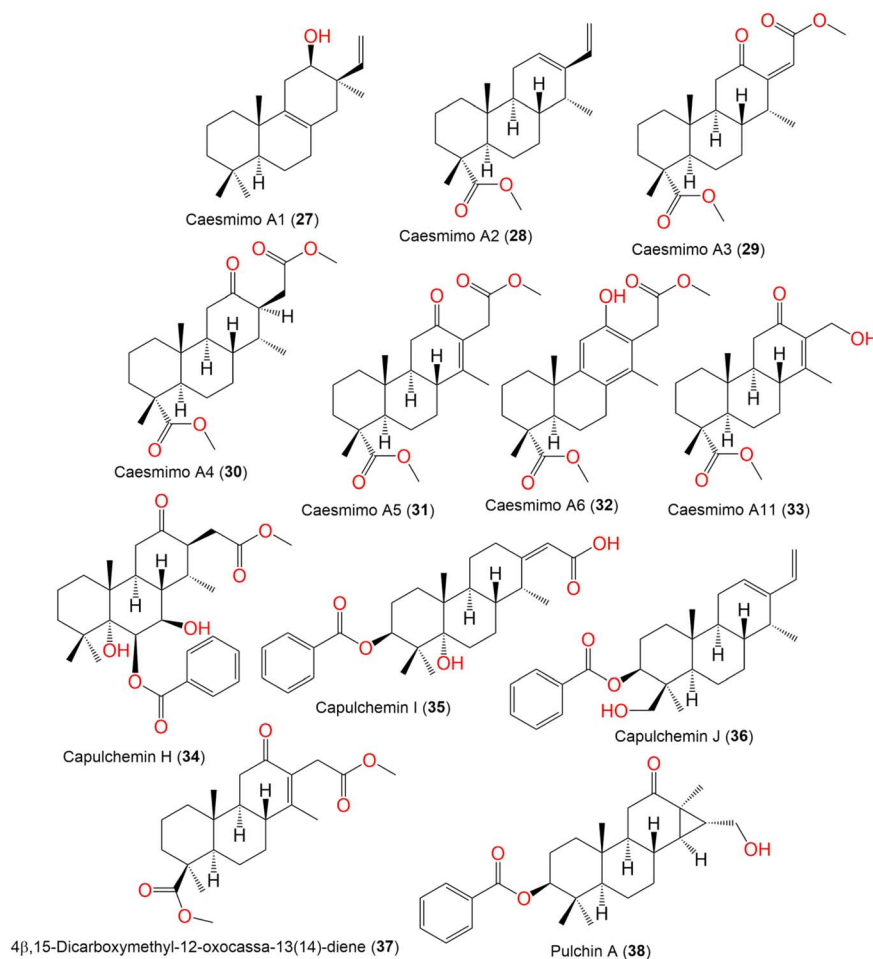


Fig. 5 Chemical structures of usual cassane diterpenoids (27–38).



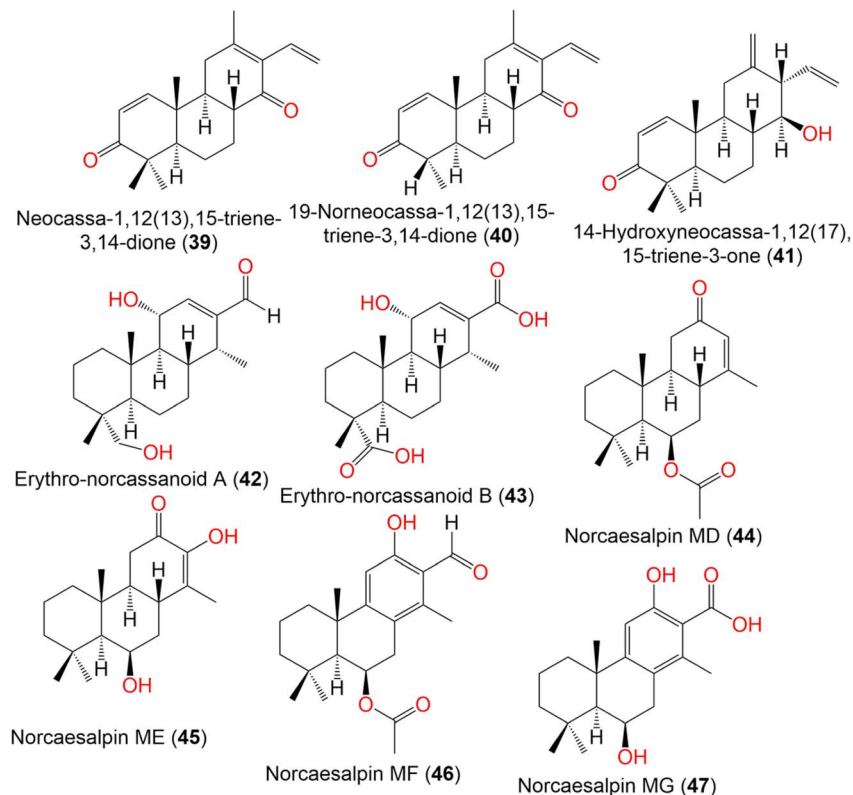


Fig. 6 Chemical structures of neocassane (39–41) and norcassane diterpenoids (42–47).

1 mg mL<sup>-1</sup>) for their phytotoxic capacities on lettuce, creeping bentgrass, and duckweed (*Lemna paucicostata* (L.) Hegelm led to the separation of 39–41 (ref. 8) (Table S3). At concentration of 1000 μM, all compounds exhibited weak phytotoxic activity, being inactive at concentrations ≥ 100 μM versus both monocot plants, particularly creeping bentgrass, with compound 41 showed the highest phytotoxic activity. Compounds 39–41 prohibited duckweed growth (IC<sub>50</sub>s 109, 200, and 59 μM, respectively), compared to atrazine (IC<sub>50</sub> 1.95 μM).<sup>8</sup> Also, they had fungicidal potential (IZDs 7.5–12.7 mm; Conc 100 μg/spot) against strawberry pathogens, including *Colletotrichum fragariae*, *Colletotrichum acutatum*, and *Colletotrichum gloeosporioides* in the bioautography TLC technique. Among them, compound 40 exhibited the strongest antifungal effect, suggesting that these neocassane diterpenoids could serve as promising bioherbicide and biocontrol agent after further investigations.<sup>8</sup>

#### 4.3. Norcassane diterpenoids

The 16-norcassane diterpenoids: 42 and 43 separated from *Erythrophleum fordii* roots by Li *et al.*, demonstrated no antiviral capacities against coxsackie and influenza viruses.<sup>28</sup> Compounds 44, 45, and 47 are norcassane diterpenoids reported from the seed kernels of *Caesalpinia sinensis*.<sup>23</sup> Among them, 44 and 45 are rare 15,16-norcassane diterpenoids, having a α,β-unsaturated carbonyl and 5*S*/6*R*/8*R*/9*S*/10*R* configuration, while 47 is a 16-norcassane derivative with aromatic ring C and a C-15-aldehyde moiety (Fig. 6). These compounds exhibited weak anti-inflammatory activity (inhibition rate 22.2–38.4%), by

prohibiting NO production induced by LPS in RAW 264.7 cells.<sup>23</sup> Further, compound 46 with 5*S*/6*R*/10*S* configuration, possesses a 16-degraded cassane skeleton with an aromatic ring C. Compound 46 showed weak inhibitory activity against NO production caused by LPS (inhibition rate 33.1%; Conc. 50 μM), in comparison to dexamethasone (inhibition rate 76.1%).<sup>32</sup>

Compound 49, a 15,16-dinorcassane diterpenoid, was isolated from the EtOAc fraction of the stem bark of *Distemonanthus benthamianus*. Its configuration was assigned as 4*R*/5*R*/6*R*/10*R*/14*S*.<sup>33</sup> It was assumed to be derived from 15*Z*-[Dodecahydro-18-hydroxymethyl-17,19,20-trimethyl-15(1*H*)-phenanthrenylidene]-acetic acid by oxidative cleavage of the C<sub>13</sub>–C<sub>15</sub> double bond, followed by oxidation and O-methylation.<sup>33</sup> Compounds 50–52 are 18,19-dinorcassane, 18-norcassane, and 15,16-dinorcassane diterpenoids, respectively (Fig. 7).<sup>29</sup>

Compound 50 is a dinorcassane bearing a C-4 ketone carbonyl, while 51 is a norcassane analogue featuring an epoxide ring. Compound 52 possesses a rare five-membered C ring. Notably, compound 50, which contains a C-4 ketone carbonyl, exhibited no anti-renal fibrosis activity in the TGF-β1-induced NRK-52E cell model, whereas compound 51, with a cyclopropane moiety at C-4, showed cytotoxicity toward NRK-52E cells.<sup>29</sup>

#### 4.4. Cassane furano-diterpenoids

Compound 53 is a 18-norcassane diterpenoid, whereas compound 54 is a rare 20-norcassane diterpenoid featuring



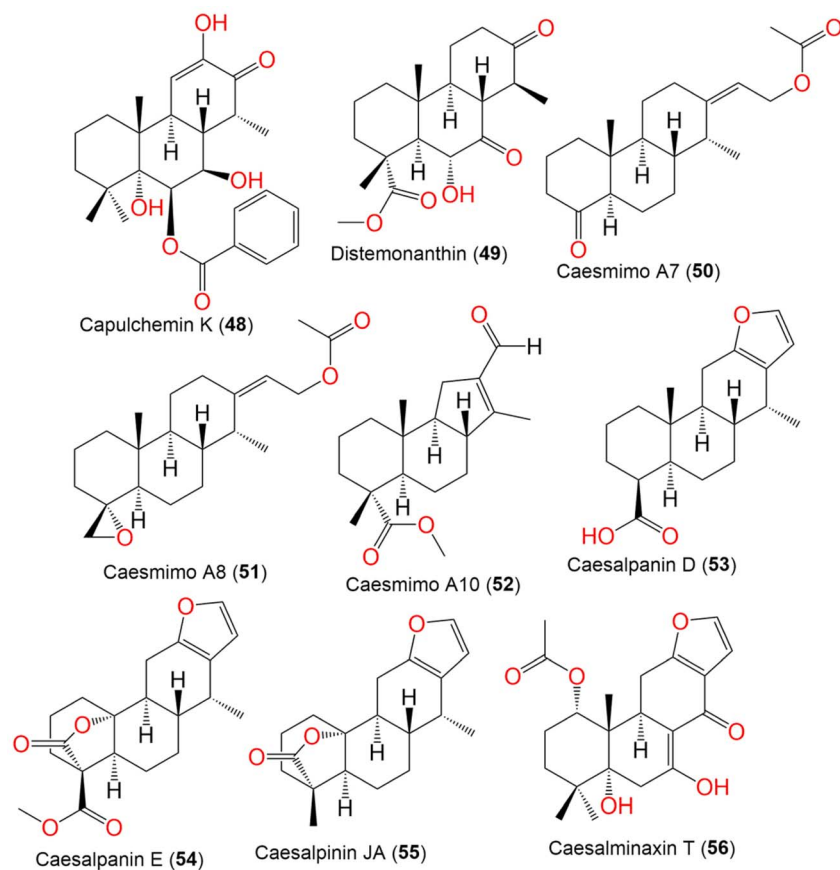


Fig. 7 Chemical structures of norcassane (48–52) and furan cassane diterpenoids (53–56).

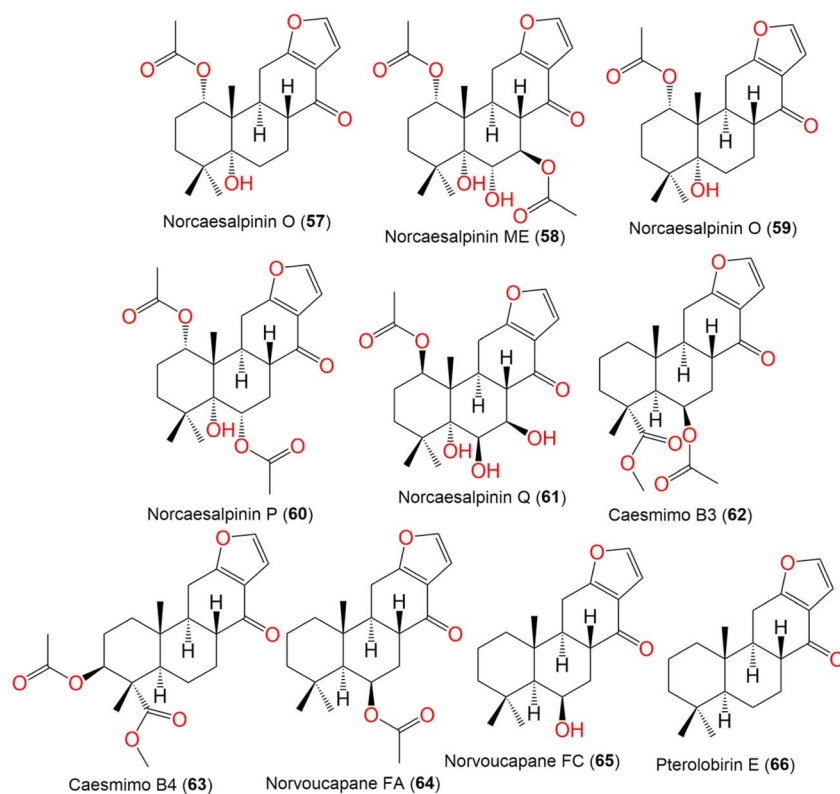


Fig. 8 Chemical structures of cassane furanoditerpenoids (57–66).

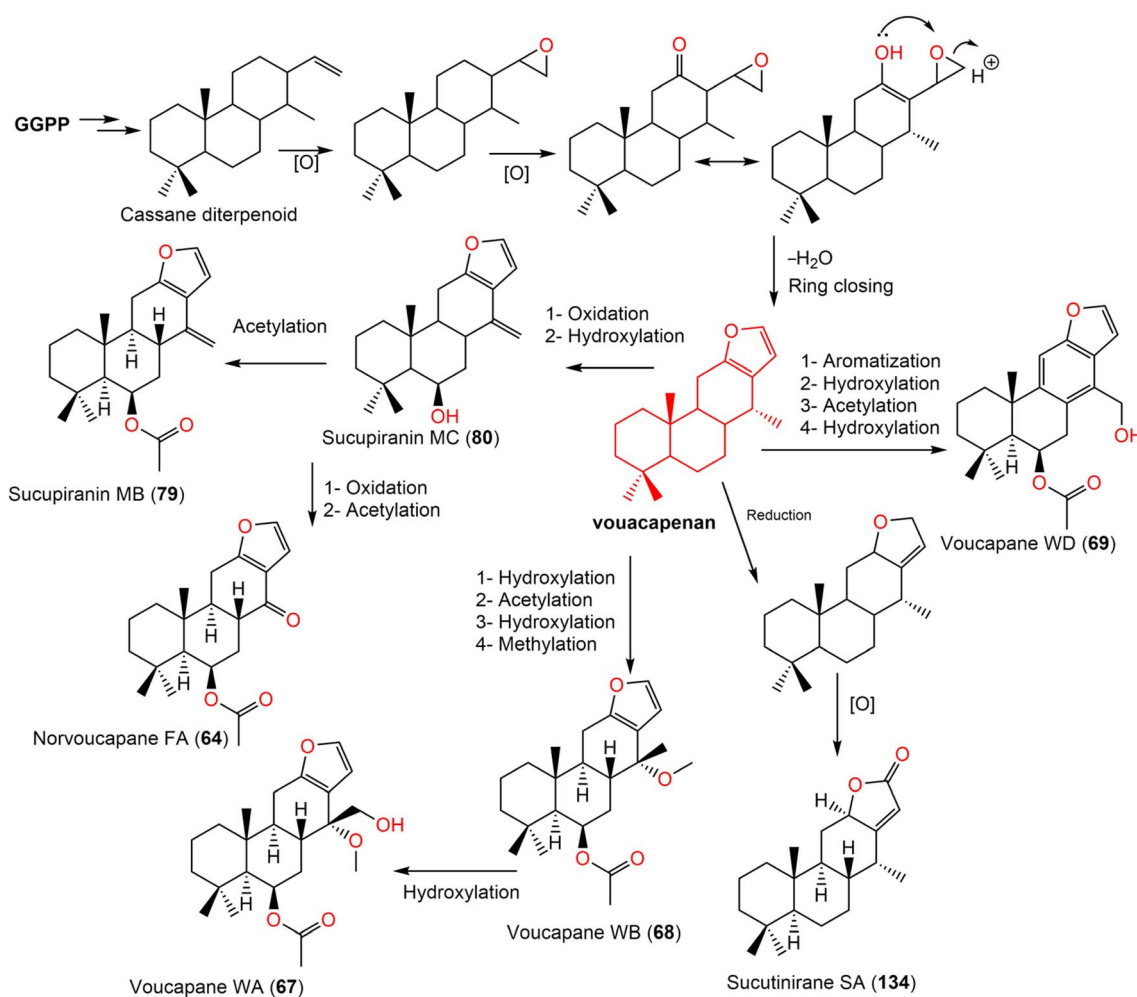


a five-membered lactone ring linking C-18 and C-10 with configurations of *4S/5S/8S/9S/10R/14R* and *4R/5S/8S/9S/10R/14R*, respectively. These two compounds were separated by Su *et al.* from *Caesalpinia sappan* seeds.<sup>34</sup> Compound 55 is an A/B *cis*-20-norcassane diterpenoid possessing a rare five-membered oxygen bridge between C-10/C-18, with *4R/5S/8S/9S/10R/14R* configuration, also isolated from *Caesalpinia sappan* seeds. It was assumed that C-20 degradation impacts the fused system. It was proposed that after C-20 decarboxylation, an intramolecular esterification occurs between C-10 and C-18, leading to the formation of a lactone ring and replacement of the  $\beta$ -COOH group by an  $\alpha$ -OH.<sup>35</sup>

Compound 56 resembles compound 24 but contains an uncommon enol group at C-7.<sup>36</sup> Compounds 59 and 60, isolated from *Caesalpinia bonduc* seed kernels, are furan cassane diterpenoids.<sup>37</sup> Compounds 59 and 60 lack the C-17 methyl, with configurations of *1S/5R/8R/9S/10S* and *1S/5R/6S/8R/9S/10S*, respectively (Fig. 8). Compound 59 demonstrated weak phosphodiesterase-4B inhibition (% inhibition 30.2% at 100  $\mu$ M), while compound 60 was weakly active.<sup>37</sup> Besides, 59 and 60 (inhibitory ratios 3.5 and 22.9%, respectively) inhibited NF- $\kappa$ B,

indicating the C-6 acetoxy group reduces inhibitory activity.<sup>37</sup> In the docking study, compound 59 displayed the same binding mode as rolipram, suggesting 59 as a potential PDE4B inhibitor.<sup>37</sup> Recently, Wang *et al.* reported that compound 62, identified from *Caesalpinia mimosoides* seeds, possessed anti-renal fibrosis activity by inhibiting fibronectin and collagen I expression induced by TGF- $\beta$ 1 (transforming growth factor- $\beta$ 1) in NRK-52E cells.<sup>38</sup> On the other hand, compounds 64 and 65, isolated from *Caesalpinia cucullata* seed kernels, suppressed LPS-induced NO formation in RAW 264.7 (inhibition ratios 30.6 and 44.4%, respectively).<sup>39</sup> Compounds 67–69, 79, and 80, also isolated from *Caesalpinia cucullata* seed kernels (Table S4), are furan diterpenoids differing in their C-14 substitution and the nature of ring C. Compounds 79 and 80 have C-14 exocyclic double bond.

These compounds suppressed LPS-induced NO formation in RAW 264.7 (inhibition ratios 26.0–66.1%). Among them, compounds 68 and 67 showed moderate anti-inflammatory activity (inhibition rates 59.5 and 66.1% at 10  $\mu$ M/L, respectively) compared to dexamethasone (inhibition rate 51.2%).<sup>39</sup> Compounds 67 notably inhibited inducible nitric oxide



Scheme 2 The plausible biosynthetic pathway of 64, 65, 67, 68, 69–80, and 134.<sup>39</sup> Drawn by the authors based on ref. 39 (original artwork; no third-party material reproduced). This article is an open access article distributed under the terms and conditions of the Creative Commons Attribution (CC BY) license.



synthase (iNOS) activation in a dose-dependent manner.<sup>39</sup> Their plausible biosynthetic pathway is illustrated in Scheme 2.<sup>39</sup>

Compounds 71–74 were obtained from the seed extract of *Caesalpinia minax*. Compound 71 with 1*S*/5*R*/6*S*/7*R*/8*S*/9*S*/10*S*/14*S* configuration is related to caesalmin Q, except for the absence of an acetyl group at C-1 and presence of one at C-6 in 71 (Fig. 9). Compound 72 has the same structure as 71, except for the interchanged positions of the 6-OH and 7-OAc groups. Compound 73 has one additional acetyl group at C-6 compared with caesalminaxin N, while 74 possesses CH<sub>2</sub>OH and OCH<sub>3</sub> at C-14 instead of HC = O and OH groups in 73. Their configurations are 1*S*/5*R*/6*S*/7*R*/8*S*/9*S*/10*S*/14*R* and 1*S*/5*R*/6*S*/7*R*/8*S*/9*S*/10*S*/14*R*, respectively. Compounds 72 displayed weak anti-inflammatory potential by inhibiting LPS-produced NO production in RAW 264.7 cells.<sup>36</sup>

Compound 77 (40 μM), reported by Huang *et al.* from *Caesalpinia minax* seeds, markedly lowered intracellular lipid

accumulation and cholesterol and total triglyceride contents in oleic acid/palmitic acid-treated AML12 hepatocytes, comparable to honokiol, suggesting its potential for treating fatty-liver disease.<sup>12</sup> New cassane diterpenoids: 75, 76, 81, and 86 were identified from *Caesalpinia bonduc* seeds (Fig. 10).<sup>40</sup>

These compounds have 5- $\alpha$ -OH and C<sub>18</sub>/C<sub>19</sub>/C<sub>20</sub> CH<sub>3</sub>, but differ in C<sub>1</sub>, C<sub>2</sub>, C<sub>6</sub>, C<sub>7</sub>, and C<sub>14</sub> substitution patterns. They were inactive (cell viability 54.35–107.03% at 40 μM) against A549, MCF-7, and HEY in the MTT method, while they weakly inhibited NO production boosted by LPS in RAW264.7 macrophages.<sup>40</sup> Jin *et al.* reported oxygen-bridged furan cassane diterpenoids, 82–84 from *C. sappan* seeds.<sup>35</sup> Compound 82 (4*R*/5*R*/8*S*/9*S*/10*R*/11*R*/14*R*/19*S*/20*R*) features two additional O-bridges among C<sub>11</sub>, C<sub>19</sub>, and C<sub>20</sub>, while compounds 83 and 84 have an ester linkage between C<sub>20</sub> and C<sub>11</sub> with configurations of 4*R*/5*R*/8*S*/9*S*/10*R*/11*R*/14*R* and 4*R*/5*R*/8*S*/9*S*/10*R*/11*R*/14*R*/20*S*, respectively.<sup>35</sup> These derivatives are biosynthetically derived from

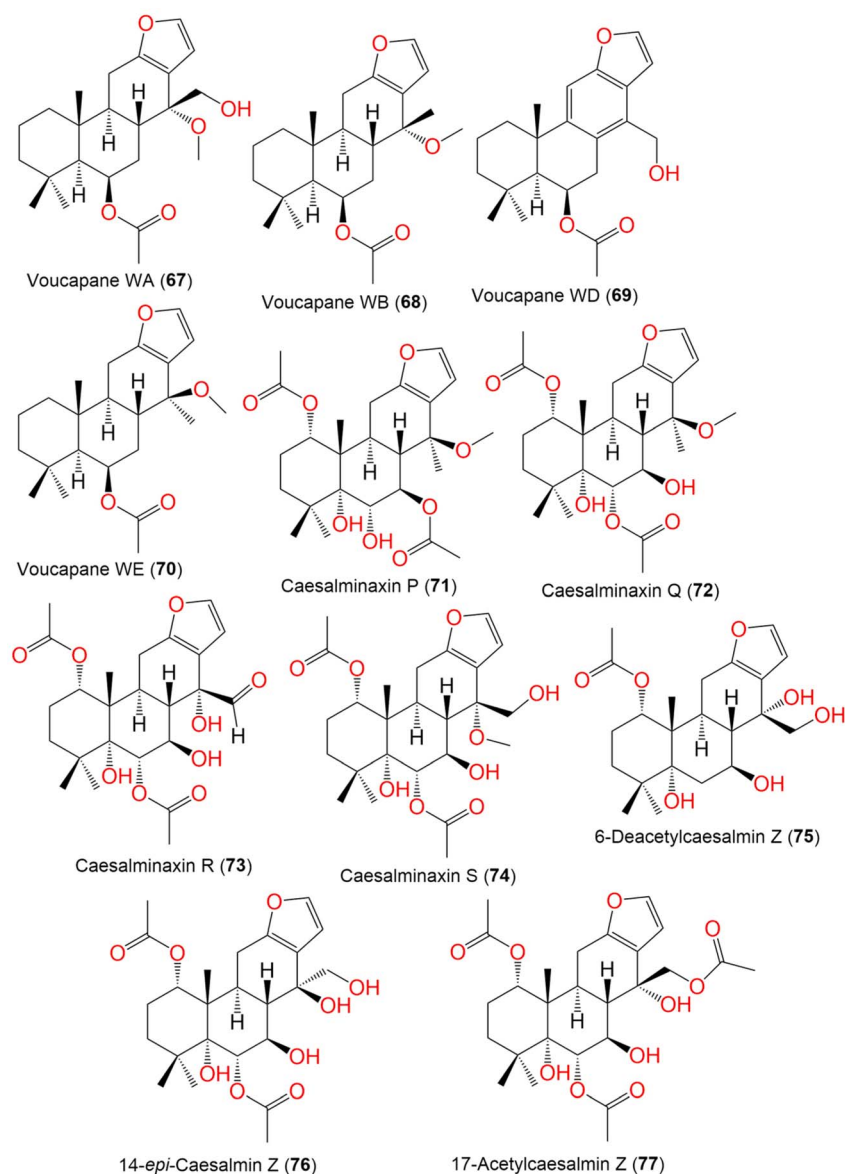


Fig. 9 Chemical structures of cassane furanoditerpenoids (67–77).



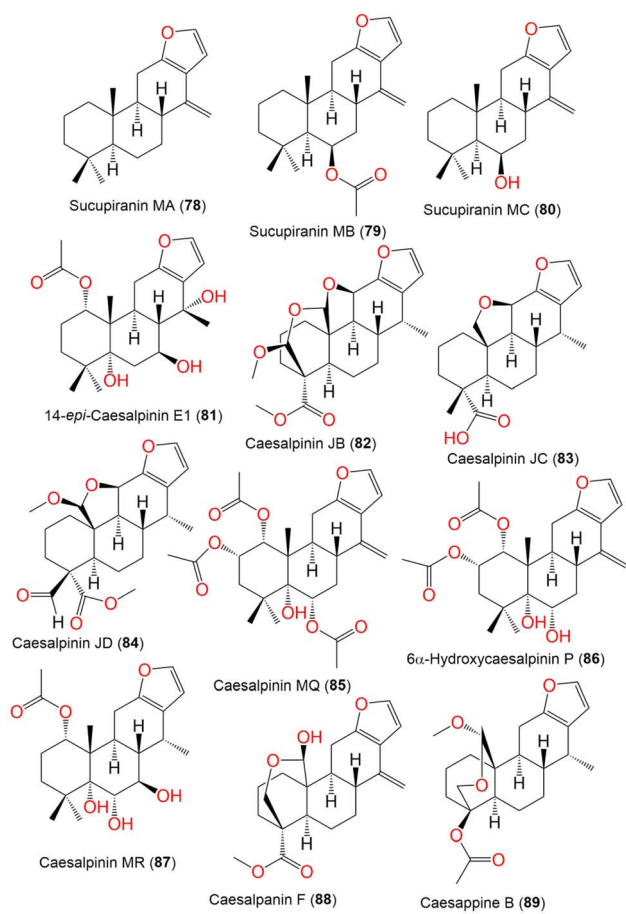


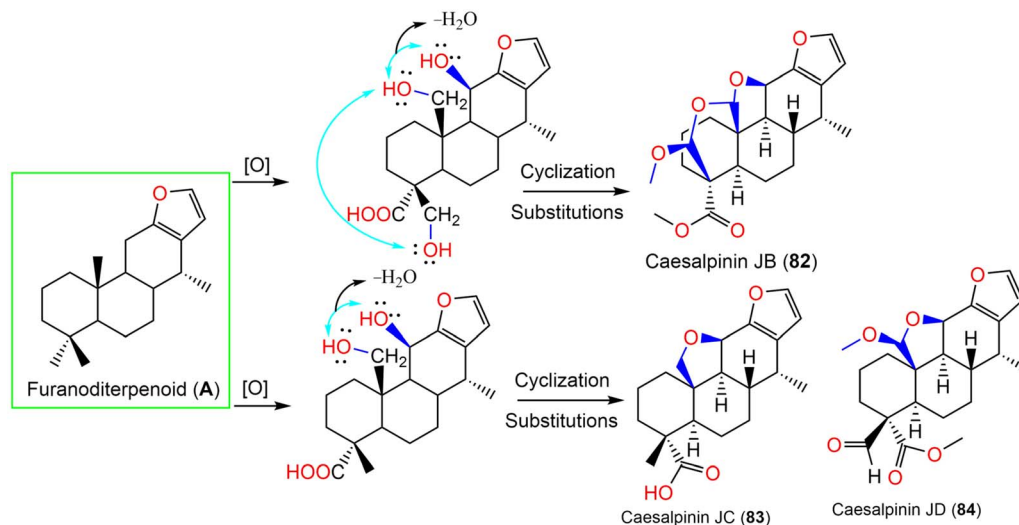
Fig. 10 Chemical structures of cassane furanoditerpenoids (78–89).

furanoditerpenoid (Scheme 3).<sup>35</sup> Compounds **82** and **84** possess an intramolecular oxygen bridge (C-11–O–C-20) formed by condensation between the C-11 hydroxyl and C-20 hydroxymethyl groups, yielding an ether/acetal linkage. Both

compounds had no cytotoxic activity against Caco-2, MCF-7, L02, HepG2, and A549 in the MTT assay.<sup>35</sup>

Compound **85** isolated from *C. bonduc*, is 1*R*/2*S*/5*R*/6*S*/8*R*/9*S*/10*S* configured and has three acetoxy groups at C-1/C-2/C-6 and C14–C17 exocyclic double bond. It showed weak phosphodiesterase-4B inhibition capacity.<sup>37</sup> Compound **88** is structurally similar to phanginin A, with replacing 14-CH and 17-CH<sub>3</sub> in phanginin A by a C-14/C-17 exocyclic double bond in **88**.<sup>41</sup> Based on comparison of its ECD spectrum with that of known cassane-type diterpenoids, the absolute configuration of **88** was assumed to be 4*R*/5*R*/8*R*/9*S*/10*S*/20*R*.<sup>34</sup> Compound **89** a cassane furanoditerpenoid containing an intramolecular acetal linkage between C-19 and C-20, showed moderate cytotoxicity toward HeLa (IC<sub>50</sub> 23.58 μM) and weak activity toward HepG-2 (IC<sub>50</sub> 53.20 μM), in comparison to cisplatin (IC<sub>50</sub>s 4.58 and 1.65 μM, respectively).<sup>41</sup> Compounds **90–95** are furano-cassane diterpenoids, possessing a rare aromatic C ring (Fig. 11).

These compounds displayed antibacterial activity against MRSA, *S. aureus*, and *Pseudomonas syringae* *pv. actinidae* (MICs 3.31–75 μM). Compound **90** had potent antibacterial properties against *S. aureus*, MRSA, *B. cereus*, and *Pseudomonas syringae* *pv. actinidae* (MICs 6.25, 6.25, 3.13, and 3.13 μM, respectively), comparable to gentamicin. Compounds **91** and **92** were active against *B. cereus* and *S. aureus* (MICs 6.25 to 12.5 μM).<sup>15</sup> Compounds **90**, **92**, and **95** with aromatic C ring, exhibited strong antifeedant potential *versus* *Plutella xylostella*, besides, **95** demonstrated more powerful antifeedant capacity against *P. xylostella* than against *M. separate* (EC<sub>50</sub> 11.98 vs. 29.11 μg cm<sup>-2</sup>).<sup>15</sup> Further, **90** significantly controlled kiwifruit canker *in vivo* through destroying the cell membrane, leading to cell death. This suggested **90** as an eco-friendly bactericide, however, further environmental and non-target safety validation is needed.<sup>15</sup> Tu *et al.* separated and identified **96–98** from *Caesalpinia minax* seeds. Compound **96** has a C<sub>23</sub> cassane diterpenoid skeleton with an unusual isopropyl moiety.



Scheme 3 Biosynthetic pathway of caesalpinins JB–JD (82–84).<sup>35</sup> Adapted from ref. 35, with permission from Elsevier. © 2022 Elsevier. License no. 6178030849466.



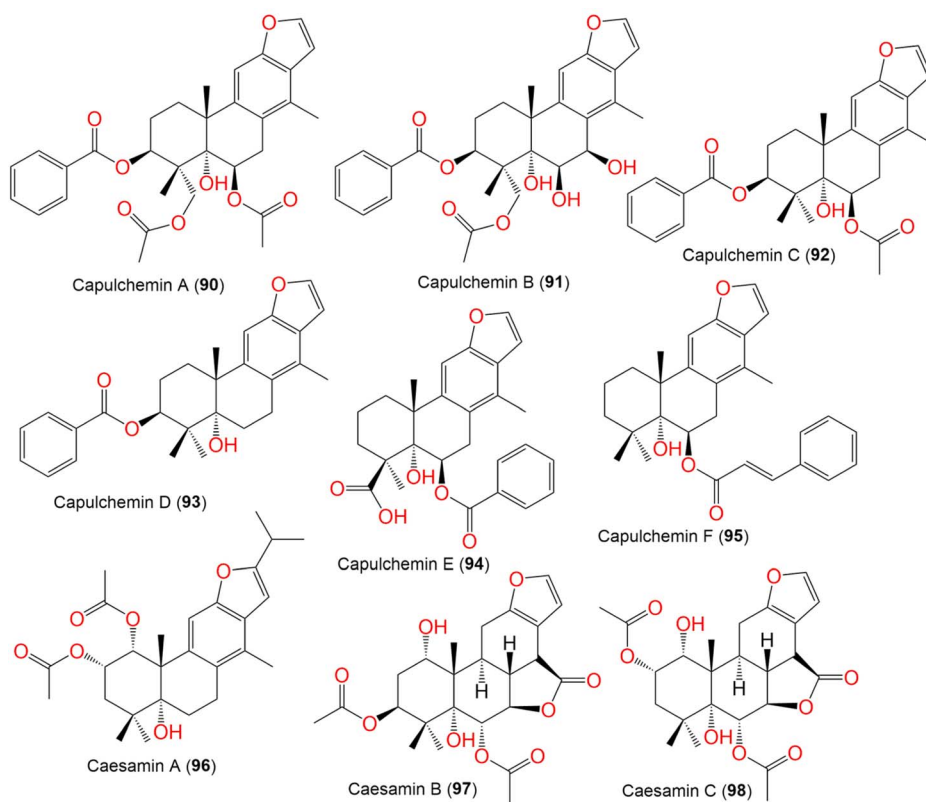


Fig. 11 Chemical structures of cassane furanoditerpenoids (90–98).

Compound **97** revealed inhibition efficacy against LPS-mediated NO production in RAW 264.7 macrophages ( $IC_{50}$  45.67  $\mu$ M), compared to NG-Monomethyl-L-arginine (43.69  $\mu$ M).<sup>42</sup> Compound **100** is a B-seco-cassane (secocassane), having a ring-opened cassane framework with a rearranged B ring, a C-7 hemiacetal and an intramolecular O-bridge reported from *P. macropterum*.<sup>43</sup> In addition to other furano-diterpenoid derivatives, **113** is a new cassane-type furanoditerpenoid with an unusual trisubstituted benzofuran moiety, two carboxymethyl groups derived from methyl oxidation and an additional acetoxy group (Fig. 12 and 13).<sup>30</sup> Compound **113** exhibited potent anti-inflammatory activity by suppressing the NO ( $IC_{50}$  7.18  $\mu$ M) production in LPS-boosted BV-2 microglial cells.<sup>30</sup>

A novel furan cassane diterpenoid, **114** was isolated from *Caesalpinia minax* seeds<sup>44</sup> that has a 21-carbons cassane diterpenoid core skeleton with an uncommon  $\alpha,\beta$ -unsaturated  $\delta$ -lactone ring. Its 1*S*/5*R*/6*S*/7*R*/8*R*/9*S*/0*S* configuration was specified by ECD quantum-chemical calculations. Biogenetically, it was assumed to originate from caesalpine C. A Claisen condensation of caesalpine C C-14 ketone carbonyl with malonyl-CoA forms I that undergoes hydrogenation, dehydration, and hydrolysis, giving II (Scheme 4). Subsequent esterification reaction between C-21 COOH and 7-OH produces **114**.<sup>44</sup> This compound accelerated wound healing by stimulating migration and tuber generation in HUVECs, attributed to upregulation of VEGF level in the CCK-8 assay.<sup>44</sup>

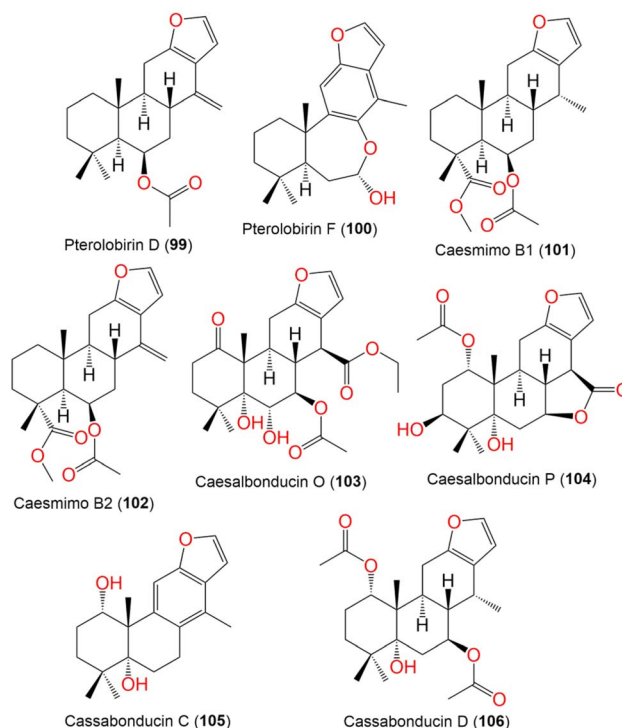


Fig. 12 Chemical structures of cassane furanoditerpenoids (99–106).



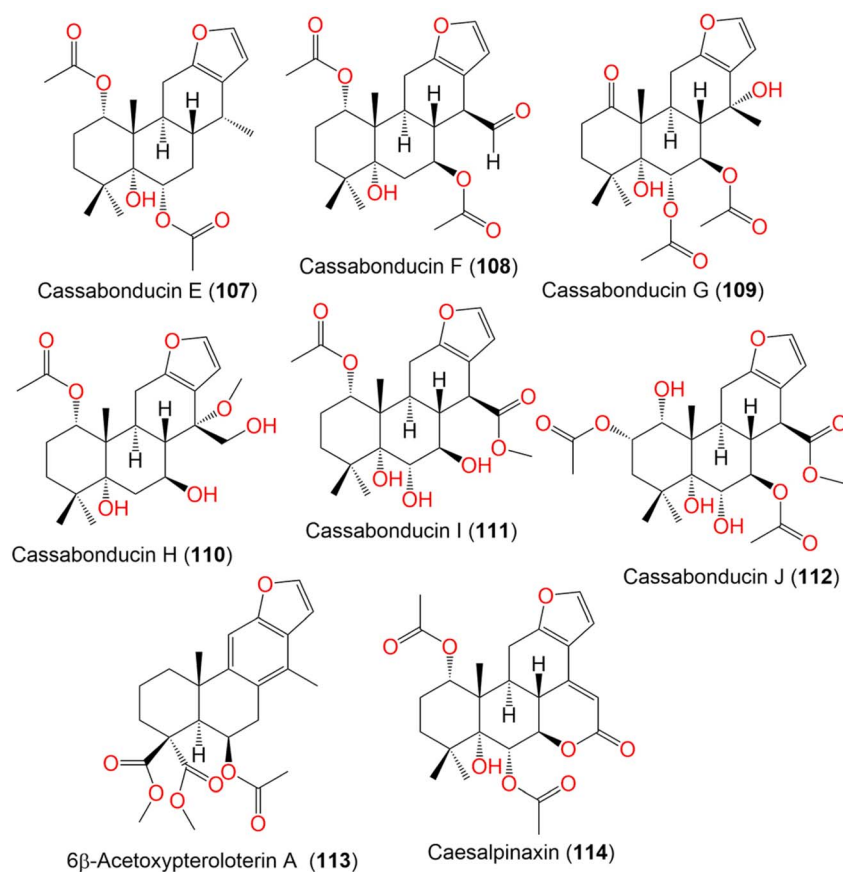
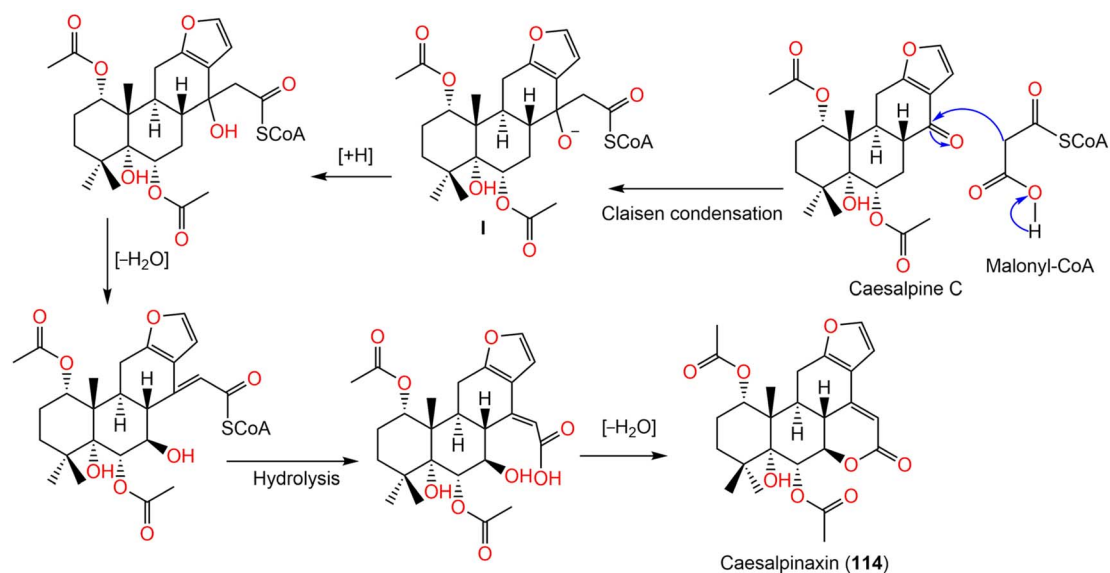


Fig. 13 Chemical structures of cassane furanoditerpenoids (107–114).

#### 4.5. Dihydrofuran cassane diterpenoids

New tetracyclic cassane diterpenoids, **115–120** bearing a C12–C15 dihydrofuran ring (C-12, C-13, C-14, C-15), were isolated from *Caesalpinia pulcherrima* aerial parts.<sup>45</sup> Compounds **115**

and **116** are C16 epimers, having C-6 benzoyloxy and C-16 methoxy substituents (Fig. 14). Also, **117** and **118** are also C16 epimers with C6-(E)-cinnamoyl instead of the benzoyloxy moiety in **115** and **116**. Compounds **115–118** are 2,5-



Scheme 4 Biosynthesis of compound **114** from caesalpine C.<sup>44</sup> Adapted from ref. 44, with permission from Elsevier. © 2021 Elsevier. License no. 6178290322021.



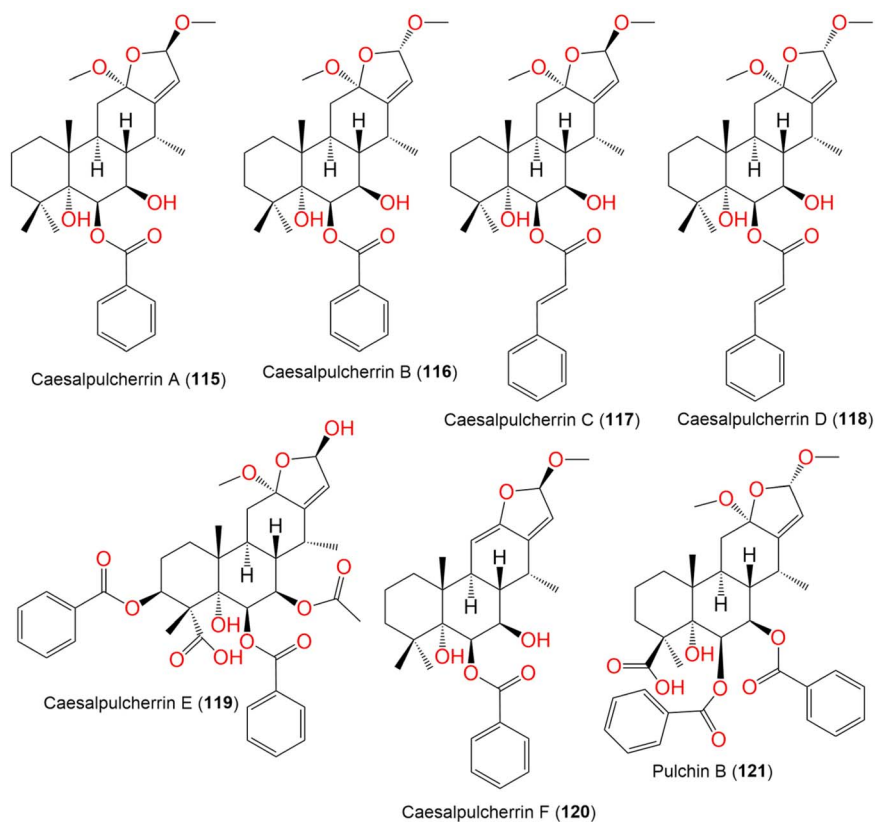


Fig. 14 Chemical structures of cassane dihydrofuran diterpenoids (115–121).

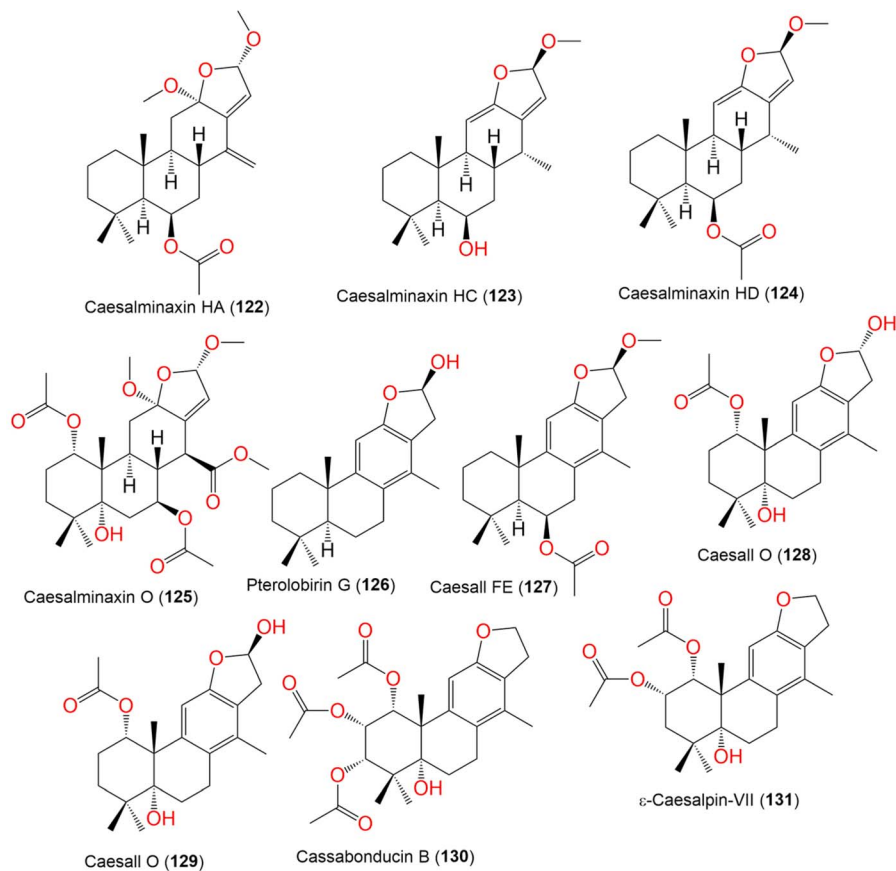


Fig. 15 Chemical structures of cassane dihydrofuran diterpenoids (122–131).



dimethoxyfuranocassane diterpenoids, while **119** is similar to **115–118** (C-6 and C-3 benzoyloxy, C-16-OH, 19-COOH, and C-7 acetoxy). Given the configurational lability at C-16, **119** may exist as C-16  $\alpha/\beta$  epimers (*cf.* **128,129**). Compound **120** is analogous to **115** with the replacement of 12-OCH<sub>3</sub> by a C<sub>11</sub>–C<sub>12</sub> double bond. Compounds **115** and **119** were assessed for anti-feedant activity against *Plutella xylostella* and *Mythimna separate* in a dual-choice bioassay. They possessed moderate anti-feedant capacity against *M. separate* (EC<sub>50</sub>s 33.54 and 24.52  $\mu\text{g cm}^{-2}$ , respectively) compared to Neem oil (EC<sub>50</sub> 4.73  $\mu\text{g cm}^{-2}$ , 1% azadirachtin).<sup>45</sup>

Compounds **123**, **124**, and **127** were obtained from *Caesalpinia sinensis* seed kernels by Li *et al.*<sup>18</sup> Compound **127** is a dihydrofuran cassane with an aromatized C ring, while **123** and **124** feature an isomerized furan ring conjugated with an additional double bond (Fig. 15).<sup>18</sup> These metabolites had no cytotoxic potential *versus* RAW 264.7 cells; however, they prohibited LPS-induced NO production in RAW 264.7 cells (% inhibition 39.6, 64.9, and 22.3%), compared to dexamethasone (76.1%).<sup>18</sup> Compound **125**, isolated from *Caesalpinia minax* seeds CHCl<sub>3</sub> fraction, is structurally similar to caesalminaxin H, with 14-OH/14-CH<sub>3</sub>, and a C-6 ethyl formate in caesalminaxin H replaced by 14-COOCH<sub>3</sub> and H atom, respectively, in **125**. Its configuration was assigned as 1*S*/5*R*/7*S*/8*R*/9*S*/10*S*/12*R*/14*S*/16*S*

based on X-ray analysis.<sup>36</sup> It exhibited no efficacy on NO production in RAW 264.7 cells induced by LPS (Conc. 100  $\mu\text{M}$ ).<sup>36</sup>

Liu *et al.* reported compounds **128** and **129** as C-16 epimers obtained as an inseparable (1 : 1) mixture from *Caesalpinia bonduc* seed kernels.<sup>37</sup> They feature dihydrofuran rings and have 1*S*/5*R*/10*S*/16*S*/*R* configurations. These compounds showed phosphodiesterase-4B and NF- $\kappa$ B inhibitory activities (Table S5).<sup>37</sup>

#### 4.6. Cassane with fused butenolide moiety

Li *et al.* isolated compound **132**, a cassane with C<sub>12</sub>–C<sub>13</sub> butenolide moiety, from *Erythrophleum fordii* roots (Fig. 16).<sup>28</sup> Compound **133** has an  $\alpha,\beta$ -butenolide moiety with 4*S*/5*R*/6*R*/8*S*/9*S*/10*R*/12*R*/14*R* configuration based on ECD analysis. Compound **133** displayed moderate anti-inflammatory activity (inhibition rate 45.8%) by suppressing NO overproduction caused by LPS, in comparison to dexamethasone (inhibition rate 76.1%).<sup>32</sup>

In 2022, Chen *et al.* reported **134–136** from *Caesalpinia sinensis* seeds (Table S6). Their configurations were assigned as 4*S*/5*R*/6*R*/8*S*/9*S*/10*R*/12*R*/14*R*, 5*S*/8*S*/9*S*/10*R*/12*R*/14*R*, and 5*S*/8*S*/9*S*/10*R*/12*R*/14*R*, respectively using ECD. These compounds were examined for *in vitro* human PTP1B (protein tyrosine phosphatase-1B) inhibition. Compound **134** demonstrated PTP1B inhibitory potential (IC<sub>50</sub> 217.45  $\mu\text{M}$ ), compared to

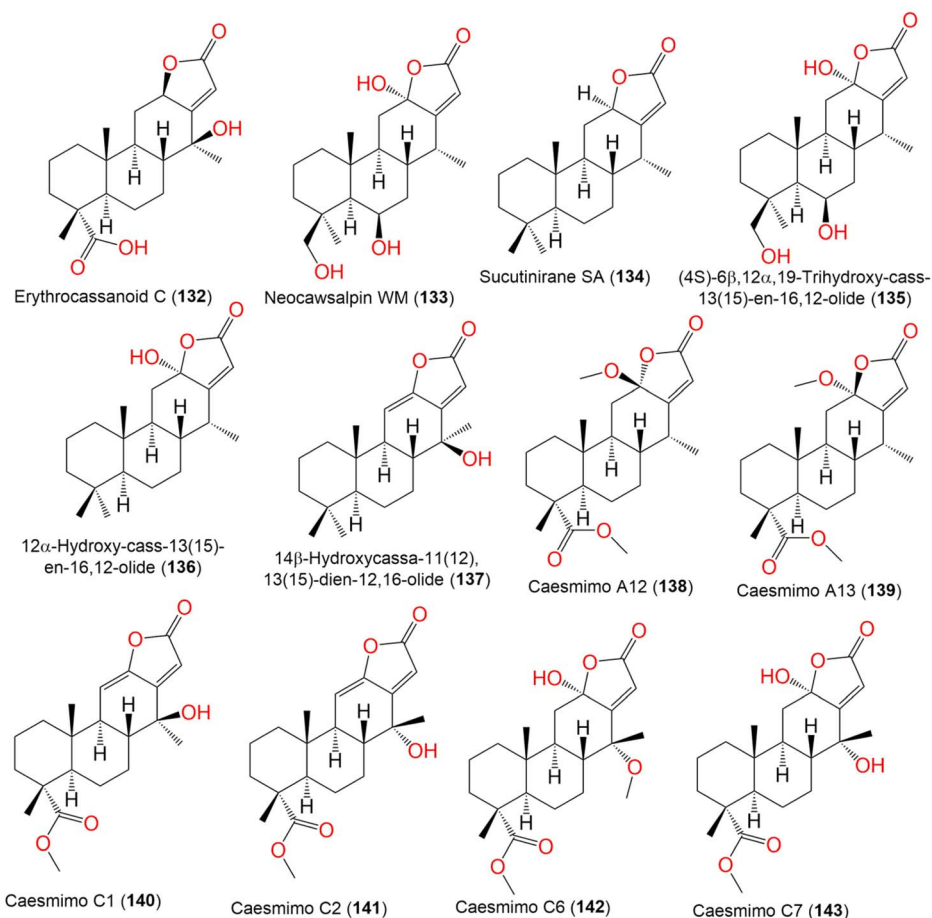


Fig. 16 Chemical structures of cassane diterpenoids with fused butenolide moiety (**132–143**).



suramin sodium ( $IC_{50}$  195.08  $\mu$ M).<sup>13</sup> Cheenpracha *et al.* isolated compound **137** from the *Pterolobium macropterum* fruits MeOH extract. Compound **137** is an  $\alpha,\beta$ -butenolide diterpenoid with a C11–C12 conjugated double bond. Compound **137** showed marked  $\alpha$ -glucosidase inhibitory capacity ( $IC_{50}$  66  $\mu$ M), compared to acarbose ( $IC_{50}$  178  $\mu$ M).<sup>6</sup> However, **138** and **139** displayed anti-renal fibrosis activity in the TGF- $\beta_1$ -induced NRK-52E model. It was found that **139** with the C-12  $\alpha$ -oriented hemiacetal OCH<sub>3</sub> had better efficacy than **138** with the  $\beta$ -oriented one.<sup>29</sup> Wang *et al.* separated **140–145** butenolide-type cassane diterpenoids from *C. mimosoides*.<sup>38</sup> Compounds **140–143** are C-14 epimer pairs, whereas **140** and **141** possess a C11–C12 double bond conjugated with an unsaturated lactone ring. Their configurations were determined as 4*R*/5*R*/8*R*/9*S*/10*R*/14*S*, 4*R*/5*R*/8*R*/9*S*/10*R*/14*R*, 4*R*/5*R*/8*R*/9*S*/10*R*/12*R*/14*R*, and 4*R*/5*R*/8*R*/

9*S*/10*R*/12*R*/14*R*, respectively using ECD analyses.<sup>38</sup> Compounds **146–150** possess  $\alpha,\beta$ -unsaturated butenolide moieties (Fig. 17).

Compounds **146** and **147** are structurally similar, with 3*S*/4*S*/5*R*/8*S*/9*S*/10*S*/12*R*/14*R* and 4*R*/5*S*/8*S*/9*S*/10*S*/12*R*/14*R* configurations, respectively. Compound **148** is 5*R*/8*S*/9*R*/10*S*/14*R*-configured with a C11–C12 conjugated double bond. Whilst **149,150** C-19 epimeric pair (19*R*/19*S*) with configurations 4*R*/5*S*/8*S*/9*S*/10*R*/12*R*/14*R*/19*R* and 4*R*/5*S*/8*S*/9*S*/10*R*/12*R*/14*R*/19*S*, respectively. Compounds **146–150** displayed cytotoxic effectiveness against A549 cell lines ( $IC_{50}$ s 16.79–28.02  $\mu$ M), compared to cisplatin ( $IC_{50}$  15.96  $\mu$ M).<sup>46</sup> Compound **146** ( $IC_{50}$  16.79  $\mu$ M) demonstrated marked antiproliferative potential in A549 cells by inducing apoptosis and suppressing the G<sub>0</sub>/G<sub>1</sub> phase of the cell cycle.<sup>46</sup> Additionally, **152**, **154–157**, and **159** are tetracyclic cassane diterpenoids with a fused butenolide moiety isolated from *Caesalpinia bonduc* seeds. All possess  $\alpha$ -5-OH and hydroxy

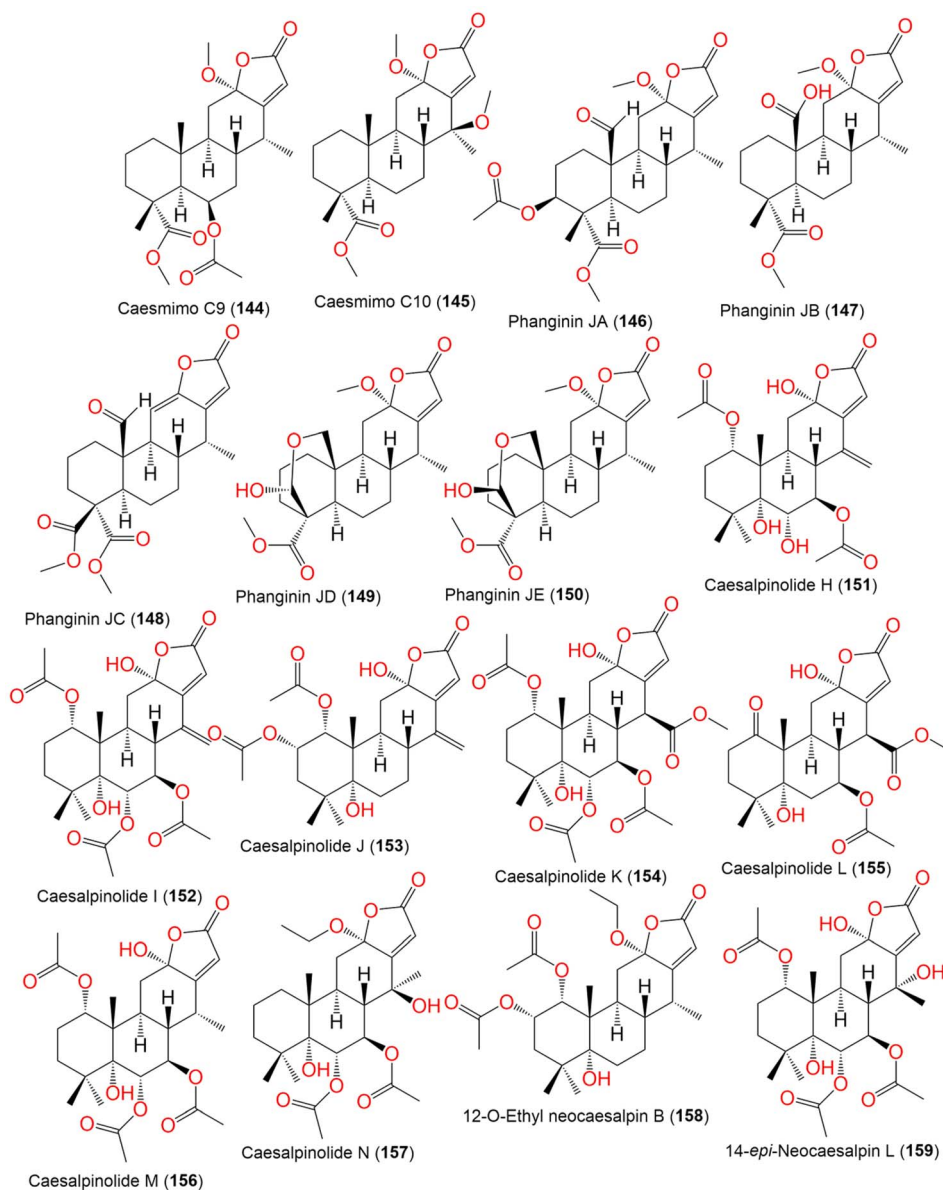


Fig. 17 Chemical structures of cassane diterpenoids with fused butenolide moiety (144–159).



or acetoxy substituents at C-1, C-6, C-7, and C-14. These compounds showed weak cytotoxic and anti-inflammatory properties.<sup>40</sup>

From 75% EtOH seed kernels extract of *Caesalpinia sinensis*, **160–171** were characterized.<sup>17</sup> These compounds contain an  $\alpha,\beta$ -butenolide ring, whereas compounds **160–162** possess a C11–C12 double bond conjugated with the unsaturated lactone ring (Fig. 18). They were weak inhibitors of LPS-stimulated NO formation in RAW 264.7 cells.<sup>17</sup>

The new tetracyclic cassane diterpenoids with fused butenolide moiety, **151, 153, 158, 172, and 173** obtained from *Caesalpinia minax* seeds showed weak cytotoxic capacities towards

A549, MCF-7 cells, and HEY cell lines.<sup>22</sup> On the other hand, **174** is 4*R*/5*R*/8*S*/9*S*/10*S*/12*R*/14*R*/19*R*/20*R* configured with 19,20-epoxide linkage (Scheme 5). It demonstrated no cytotoxic capacity versus different cell lines.<sup>35</sup>

Compounds **176–178** are new cassane diterpenes with an  $\alpha,\beta$ -unsaturated lactone moiety separated by Li *et al.* (2020b) from *C. pulcherrima* aerial parts. Compound **177** is similar to **176**, with the absence of C-6-benzoyloxy and C-7 acetoxy groups and having C-12 methoxy and C-4 methyl instead of C-17 hydroxyl and C-4 carboxyl in **176**. Compound **178** was reported for the first time as a natural product. Compounds **176** and **178** showed antifeedant activity against *Mythimna separate*

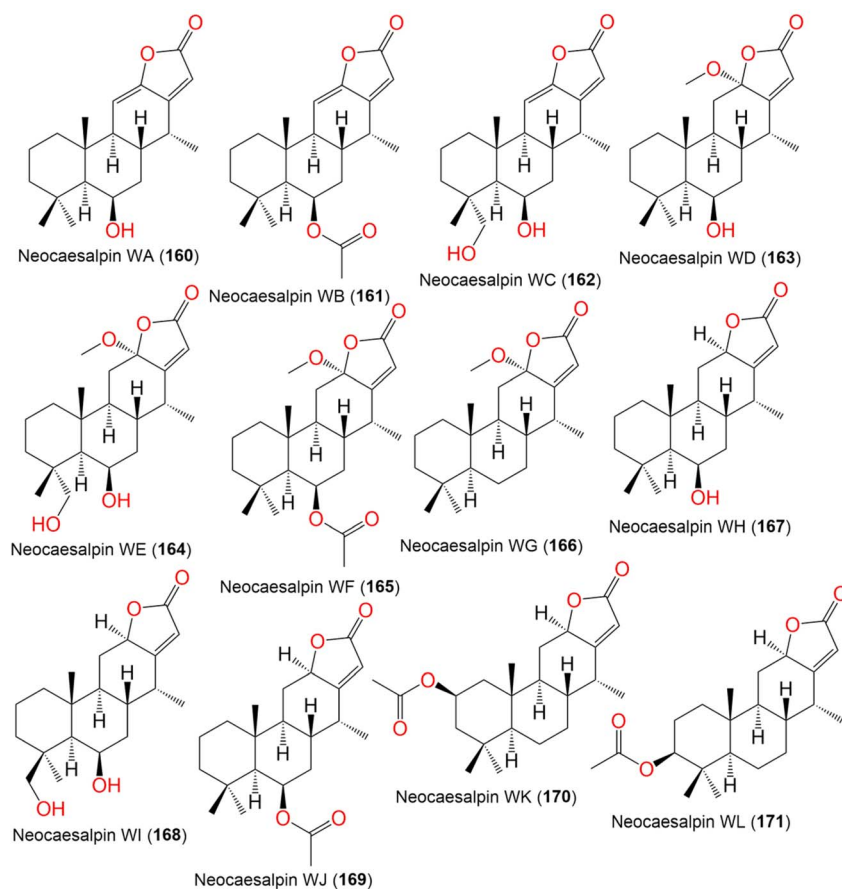
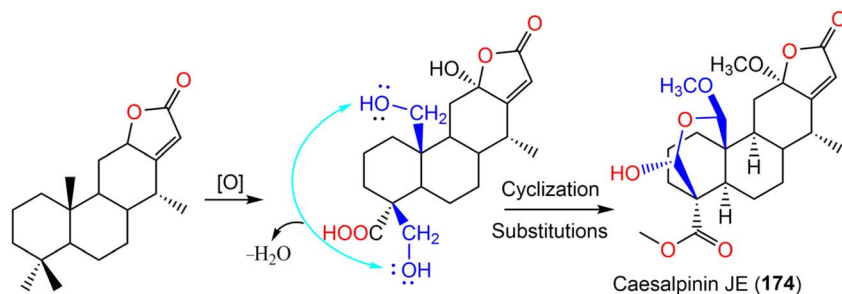


Fig. 18 Chemical structures of cassane diterpenoids with fused butenolide moiety (**160–171**).



Scheme 5 Biosynthetic pathway of compound **174**.<sup>35</sup> Adapted from ref. 35, with permission from Elsevier. © 2022 Elsevier. License no. 6178030849466.



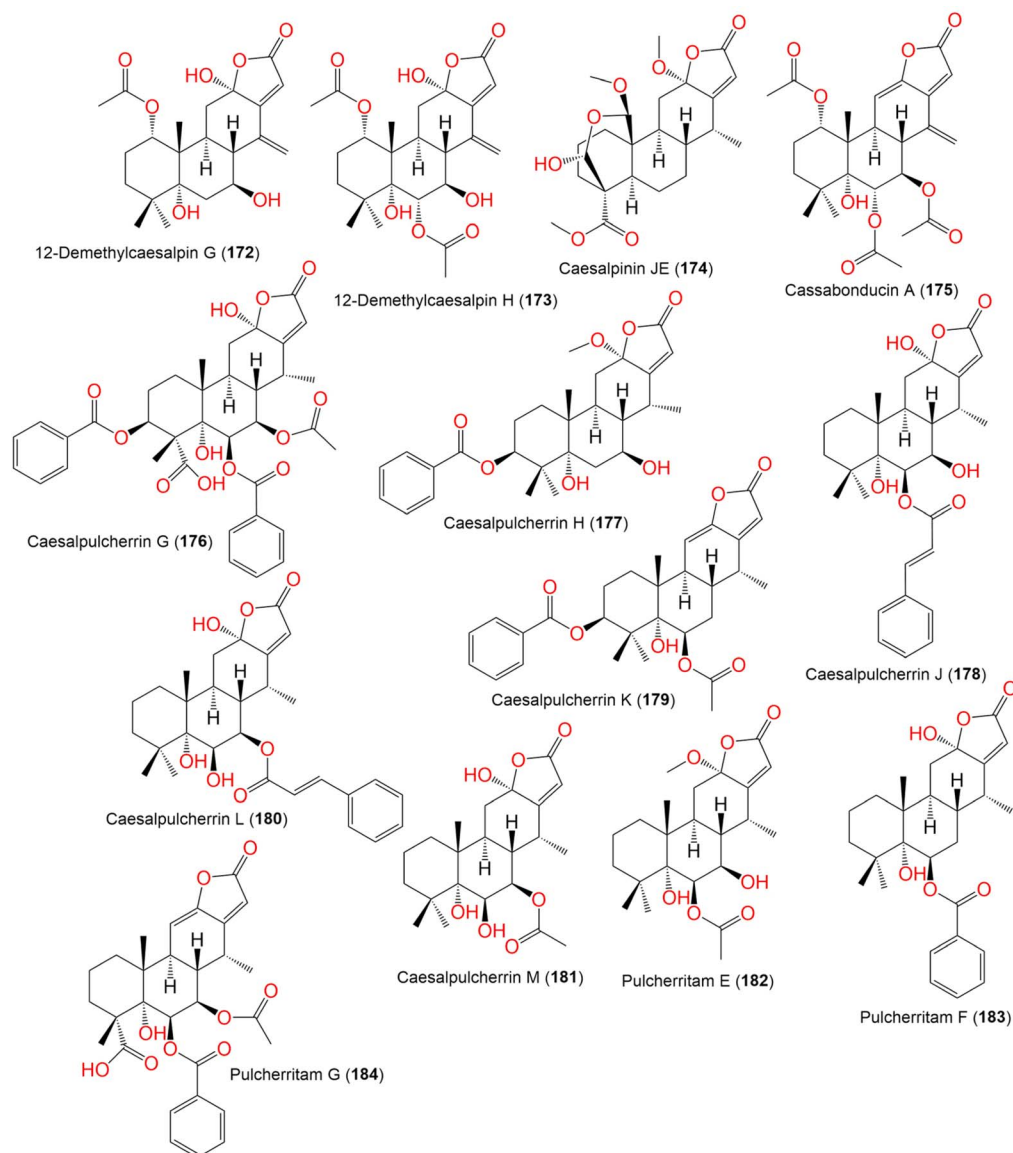


Fig. 19 Chemical structures of cassane diterpenoids with fused butenolide moiety (172–184).

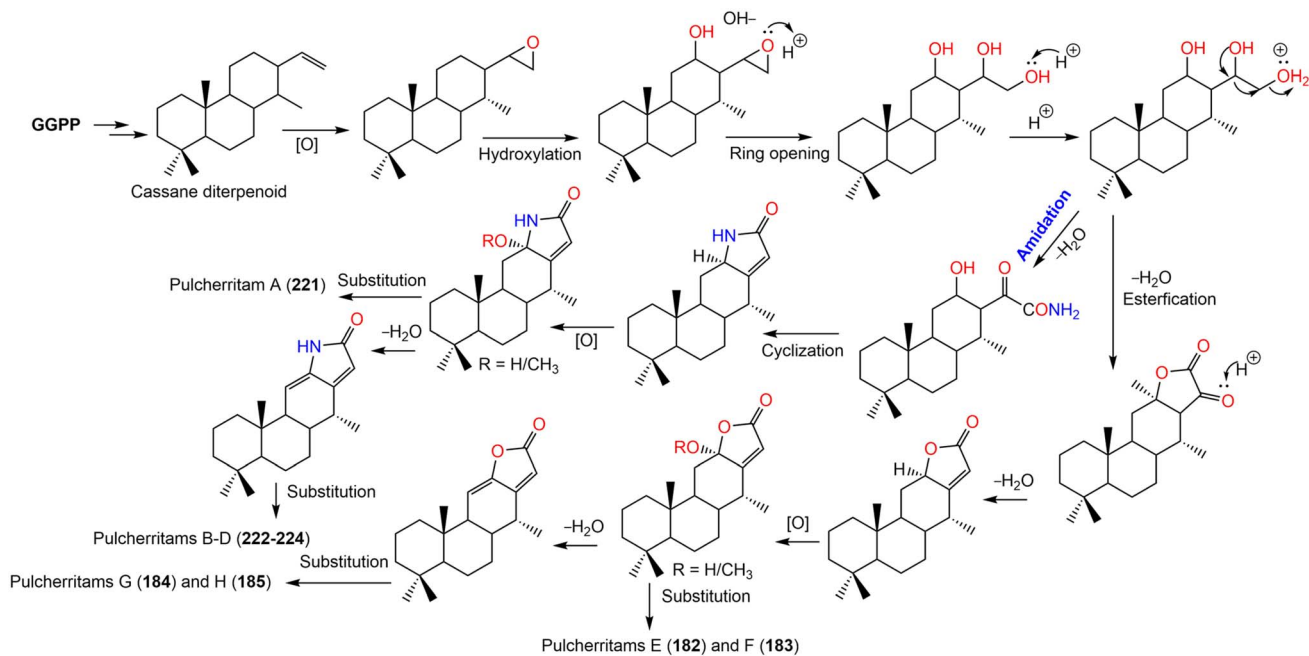
and *P. xylostella* in the dual-choice bioassay ( $EC_{50}$  49.11 and 5.06  $\mu\text{g cm}^{-2}$  and 11.84 and 15.74  $\mu\text{g cm}^{-2}$ , respectively), compared with Neem oil (1% azadirachtin,  $EC_{50}$  4.73 and 3.61  $\mu\text{g cm}^{-2}$ , respectively). Besides, 178 had moderate insecticidal activity against *M. separate* (CM (corrected mortality) 48.3%), compared to podophyllotoxin (CM 82.3%).<sup>45</sup> Yun *et al.* separated 179–181 from *Caesalpinia pulcherrima* aerial parts. Compound 179 has a C-11 and C-12 olefin bond (Fig. 19). These compounds had moderate inhibitory properties ( $IC_{50}$ s 6.34, 6.04, and 6.48  $\mu\text{M}$ , respectively) against LPS-induced NO production in BV-2 microglial cells, compared to quercetin ( $IC_{50}$  2.4  $\mu\text{M}$ ), while they displayed no  $\alpha$ -glucosidase activities.<sup>47</sup> Compounds 182–185 obtained from *C. pulcherrima* aerial parts showed weak antibacterial activity in the broth microdilution assay,<sup>14</sup> except 185 was active against *B. cereus*, *Pseudomonas syringae* pv. *Actinidae*, and *S. aureus* (MICs 6.25, 12.5, and 6.25

$\mu\text{M/L}$ , respectively), compared with gentamicin (MICs 12.5, 1.25, and 12.5  $\mu\text{M/L}$  respectively).<sup>14</sup> Besides, they had weak anti-glioblastoma activity against U87MG cells ( $IC_{50}$  27.3–35.2  $\mu\text{M}$ ).<sup>14</sup>

Biosynthetically, these compounds were assumed to be biosynthesized *via* oxidation, hydroxylation, and ring-seco of the cassane diterpenoid. Compounds 182–185 are formed through different reactions, including esterification, hydroxylation, and subsequent oxidation. For the lactam series (221–224), nitrogen is introduced after acyl activation *via* an amidation step, followed by intramolecular  $\gamma$ -lactam formation (Scheme 6).<sup>14</sup>

Compounds 186 and 187, isolated from *Caesalpinia latifolia* (Cav.) Hattink leaves, feature a C6-iso-pentanoyloxy moiety (Fig. 20).<sup>48</sup> Compound 188, a cassane lactone diterpenoid with cleavage of the C-ring, was separated from *Caesalpinia sappan* seeds. It possessed cytotoxic effect against HepG and HeLa ( $IC_{50}$ s 25.63 and 11.42  $\mu\text{M}$ , respectively),





Scheme 6 Biosynthetic pathways of compounds 182–185 and 221–224.<sup>14</sup> Adapted from ref. 14, with permission from Elsevier. © 2022 Elsevier. Licence no. 6178290696262.

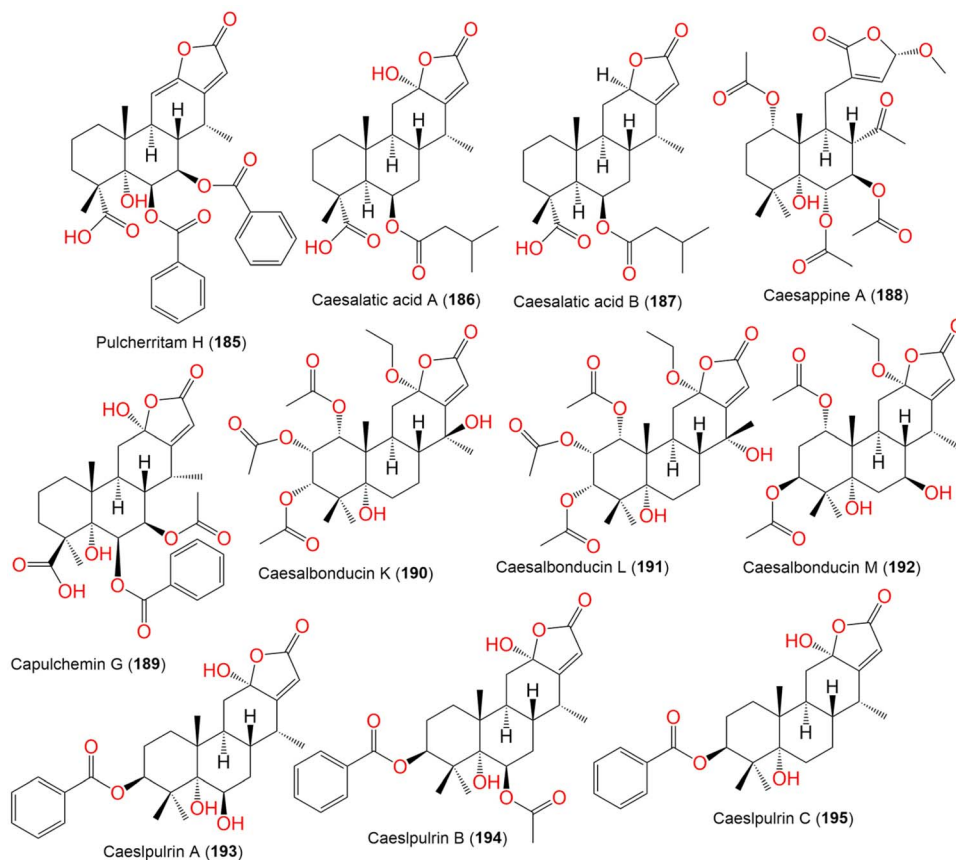


Fig. 20 Chemical structures of cassane diterpenoids with fused butenolide moiety (185–195).



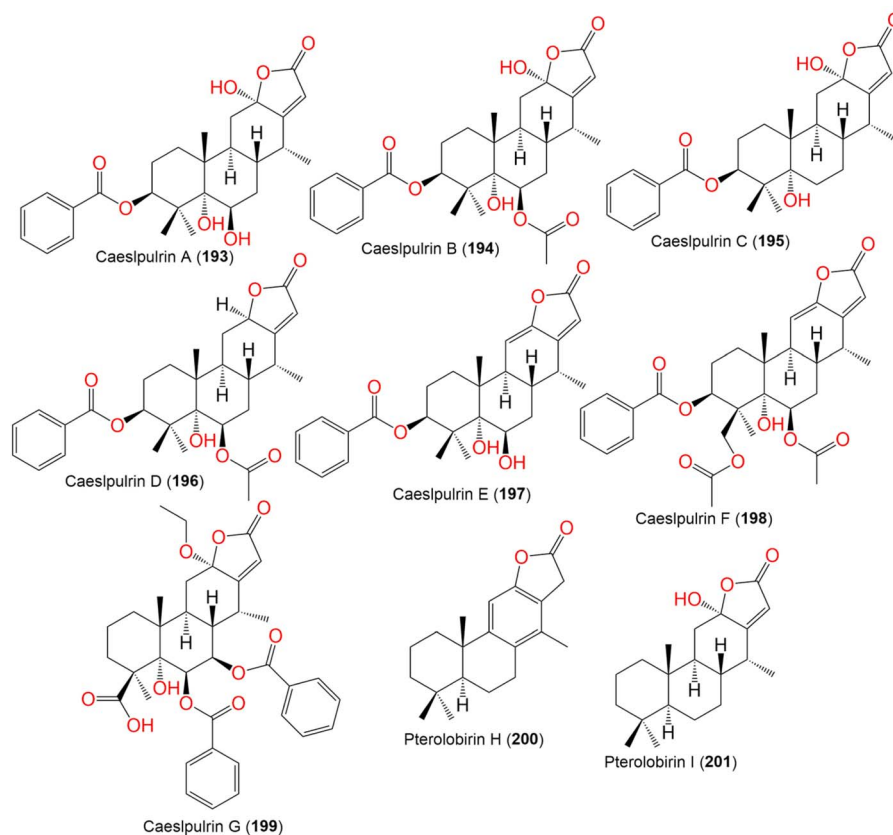


Fig. 21 Chemical structures of cassane diterpenoids with fused butenolide moiety (196–201).

compared to cisplatin ( $IC_{50}$ s 4.58 and 1.65  $\mu$ M, respectively) in the MTT assay.<sup>41</sup>

Compounds **193–199** were isolated from *Caesalpinia pulcherrima* fruits. Among them, **193–198** are rare cassane butenolides with a C-3 benzoyloxy unit (Fig. 21). Compounds **193–199** demonstrated weak inhibitory properties on LPS-induced NO production in RAW 264.7 macrophages. Additionally, **193**, **195**, and **196** with hemiketal C-12-OH had *in vitro* inhibitory potential against K-562, A-549, HepG-2, and SW-480 (inhibition ratio 53.00–88.78%), revealing C-12-OH is essential for their inhibitory activities.<sup>49</sup>

#### 4.7. Dimeric and penta-spirocassane diterpenoids

Some occurring cassane diterpenoids reported from the *Caesalpinia* genus occur as dimers (C–O or C–C linked) or Diels–Alder adducts. Raksat *et al.* reported **202** and **203**, two dimeric cassane diterpenoids with an uncommon 6/6/6/6/6/5/6/6/6 nonacyclic framework from *P. macropterum* fruits MeOH extract (Fig. 22). These are Diels–Alder adducts with unprecedented bridged 1,3-dioxan-4-one and 6/6/5 tricyclic rings.

These compounds were proposed to result from the coupling of vouacapanone (as dienophile) and taepenin K (as diene) (Scheme 7). Their 6/6/6/6/6/5/6/6/6 nonacyclic core forms through intramolecular nucleophilic addition and intermolecular Diels–Alder reaction.<sup>5</sup>

Compound **204** is a dimeric caged-cassane diterpenoid with an uncommon 6/6/6/6/6/5/6/6/6 nonacyclic ring skeleton isolated from *P. macropterum* fruits MeOH extract (Table S7). Compound **204** ( $IC_{50}$  44  $\mu$ M) demonstrated more powerful glucosidase inhibition capacity than acarbose ( $IC_{50}$  178  $\mu$ M).<sup>6</sup>

Xu *et al.* reported the isolation of **206** and **207** from *C. minax*.<sup>50</sup> These compounds are highly oxidized dimeric cassane diterpenoids, having a new alicyclic skeleton by a cyclohexene ring through intermolecular [4 + 2] Diels–Alder cycloaddition, forming a heptane-ring framework. The two diterpene parts are linked by this cyclohexene ring, which is formed by the simultaneous production of a diene (C-15–C-13–C14–C17) of one cassane moiety and mono-substituted alkene (C-15'–C-16') of the other.<sup>50</sup> It was postulated that furan rings in caesalmins B and C are oxidized and opened to give I and II, respectively. A [4 + 2] cycloaddition between the diene and a mono-substituted alkene results in a cyclohexene ring, which undergoes further oxidation to provide **206**. Compound **207** similarly arises from caesalpinin ME and caesalmin M (Scheme 8).<sup>50</sup>

These metabolites, **206** and **207** showed potent anti-inflammatory activity by suppressing LPS-caused NO formation in THP-1 macrophages ( $IC_{50}$ s 1.20 and 2.30  $\mu$ M/L, respectively).<sup>50</sup> Additionally, **206** prohibited macrophage migration towards adipocytes and suppressed NLRP3 inflammasome-mediated IL-1 $\beta$  production, alleviating inflammation of adipose tissue *via* prohibiting macrophage accumulation, suggesting their potential for treating adipose tissue inflammation



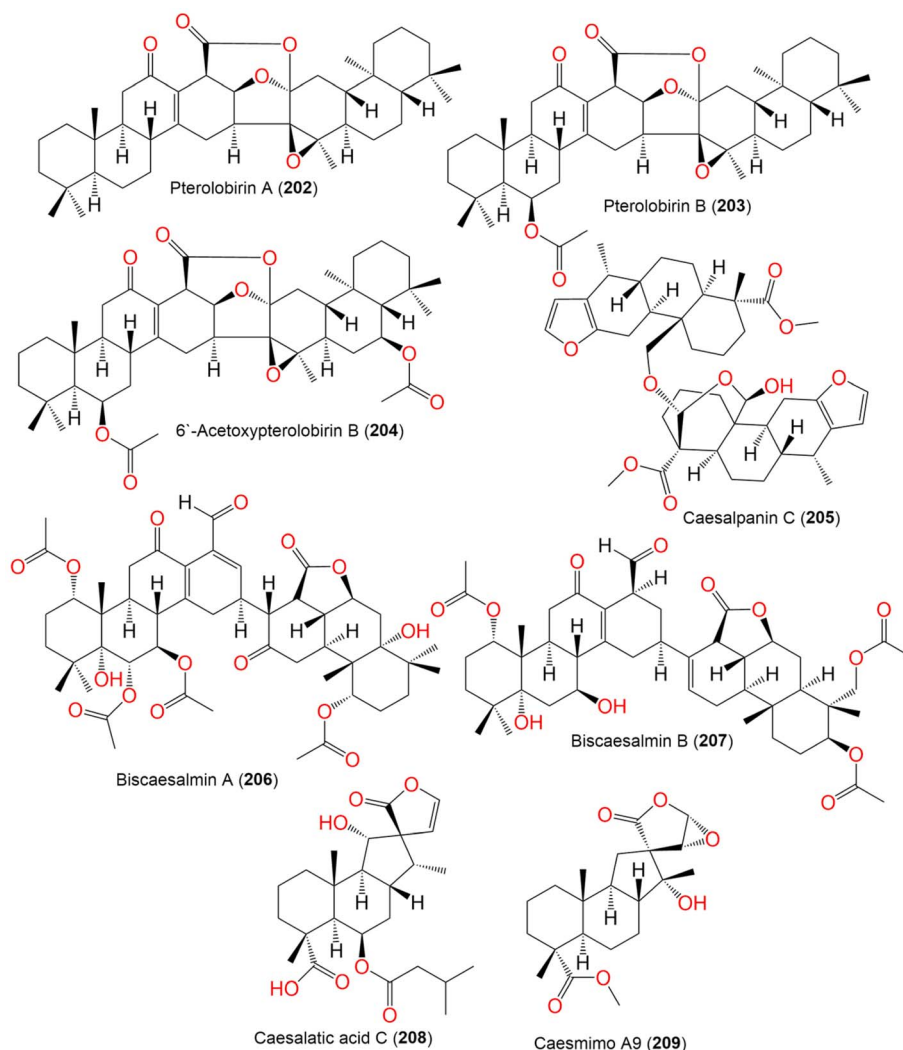


Fig. 22 Chemical structures of dimers (202–207) and penta-spirocassane diterpenoids (208 and 209).

and associated metabolic diseases.<sup>50</sup> Additionally, **208** isolated from *C. latisiliqua* leaves, features a C6-*iso*-pentanoyloxy moiety and a  $\gamma$ -spiro lactone moiety at C-13.<sup>48</sup> In 2022, Zhang *et al.* reported **209**, a rare penta-spiro cassane diterpenoid with 4*R*/5*R*/8*R*/9*S*/10*R*/12*R*/14*R*/15*R*/16*S* configuration from *C. mimosoides*.<sup>29</sup>

#### 4.8. Cassane diterpenoid alkaloids

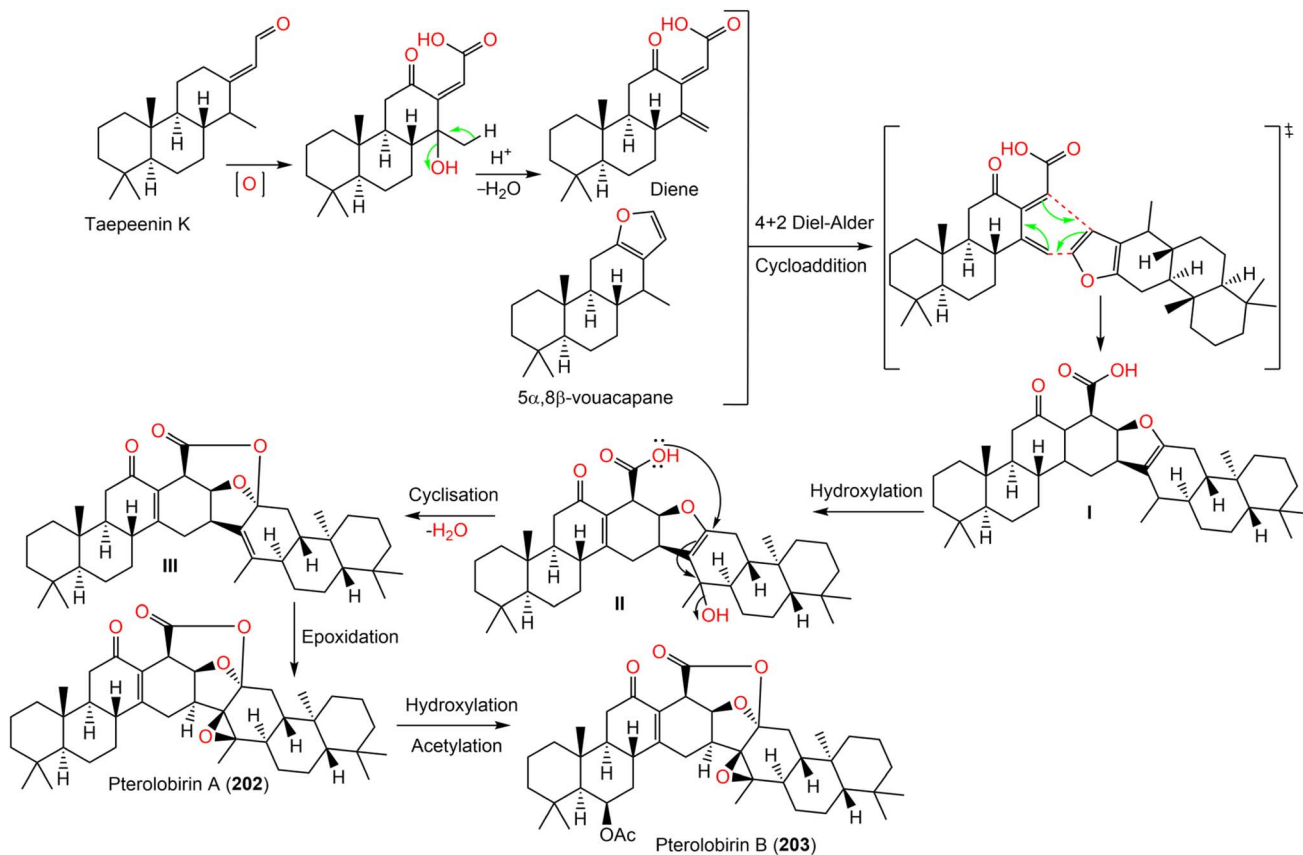
Wang *et al.* identified rare cassane diterpenoids with  $\alpha,\beta$ -unsaturated  $\gamma$ -lactam D-ring conjugated with an additional double bond: **210–214** from *Caesalpinia sinensis* seed kernels (Fig. 23). These compounds suppressed the NO production (IC<sub>50</sub>s 8.2, 9.8, and 11.2  $\mu$ M, respectively), compared to dexamethasone (IC<sub>50</sub> 0.58  $\mu$ M).<sup>17</sup>

Further, **210** was found to downregulate iNOS protein expression and lessen iNOS enzyme activity, leading to suppressing the excessive NO production.<sup>17</sup> Docking study by Wang *et al.* revealed its strong iNOS binding ( $\Delta G$   $-9.5$  kcal mol<sup>-1</sup>); the  $\alpha,\beta$ -unsaturated  $\gamma$ -lactam engaged Phe-363 and Pro-344 *via* H-bonds and Hem-901 *via*  $\pi$ - $\pi$  T-shaped contact, suggesting the  $\alpha,\beta$ -unsaturated  $\gamma$ -lactam ring has a substantial role in the anti-

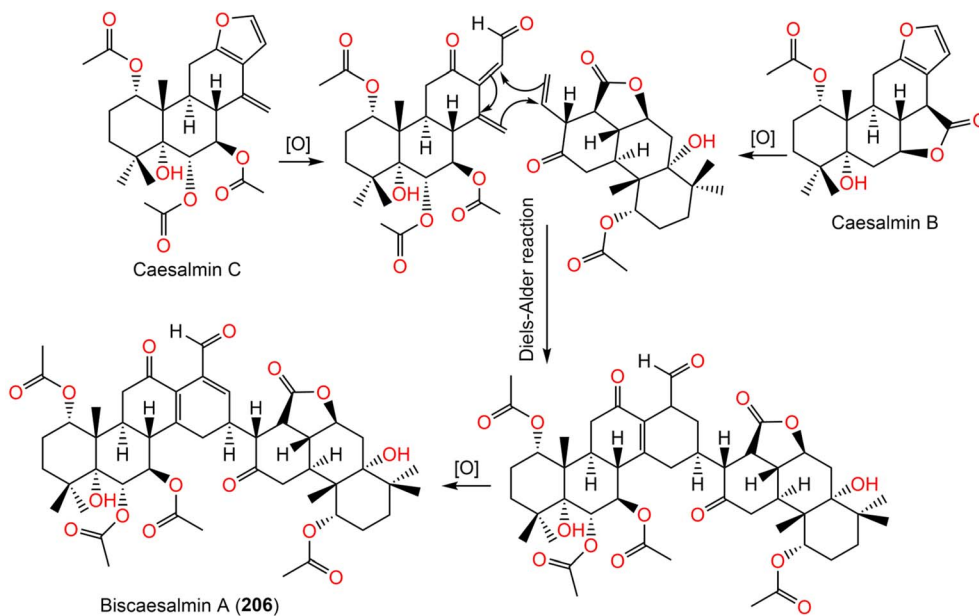
inflammatory activity.<sup>17</sup> Their postulated biosynthetic pathway begins with geranylgeranyl pyrophosphate that yields intermediate **1**, through oxidation, hydroxylation, ring-opening, and dehydration reactions. The lactone cassane skeleton is generated from **1** *via* esterification reactions (Scheme 9).<sup>17</sup> For the lactam series, the side-chain carboxylate undergoes acyl activation followed by amination (N introduction) and intramolecular  $\gamma$ -lactam cyclization.

Compounds **216–220**, new cassane alkaloids with a lactam D-ring were separated from *C. bonduc* pericarp.<sup>51</sup> These compounds were inactive against U87MG, A-431, and A-549 cell lines in the sulforhodamine B method.<sup>51</sup> Compounds **221–224** with  $\alpha,\beta$ -unsaturated  $\gamma$ -lactam ring were separated from *C. pulcherrima* aerial parts.<sup>14</sup> They have 5*R*/6*R*/7*R*/8*S*/9*S*/10*R*/12*R*/14*R* configurations; compounds **221** and **223** possess a 6-benzoyloxy moiety, and **222** has an (*E*)-cinnamoyl moiety (Fig. 24). Compounds **221** and **222** (MICs 75.0 and 25.0  $\mu$ M/L, respectively) displayed antibacterial potential against *Erwinia carotovora* subsp. *Carotovora* and MRSA, compared with gentamicin (MICs 12.5 and 50.0  $\mu$ M/L, respectively).<sup>14</sup>





Scheme 7 Biosynthetic pathway of compounds 202 and 203.<sup>5</sup> Adapted from ref. 5, with permission from the American Chemical Society. © 2020 American Chemical Society. License no. 6178291080474.



Scheme 8 Biosynthetic pathway of 206 from caesalmins B and C.<sup>50</sup> Adapted from ref. 50, with permission from Elsevier. © 2021 Elsevier. License no. 6178300090790.



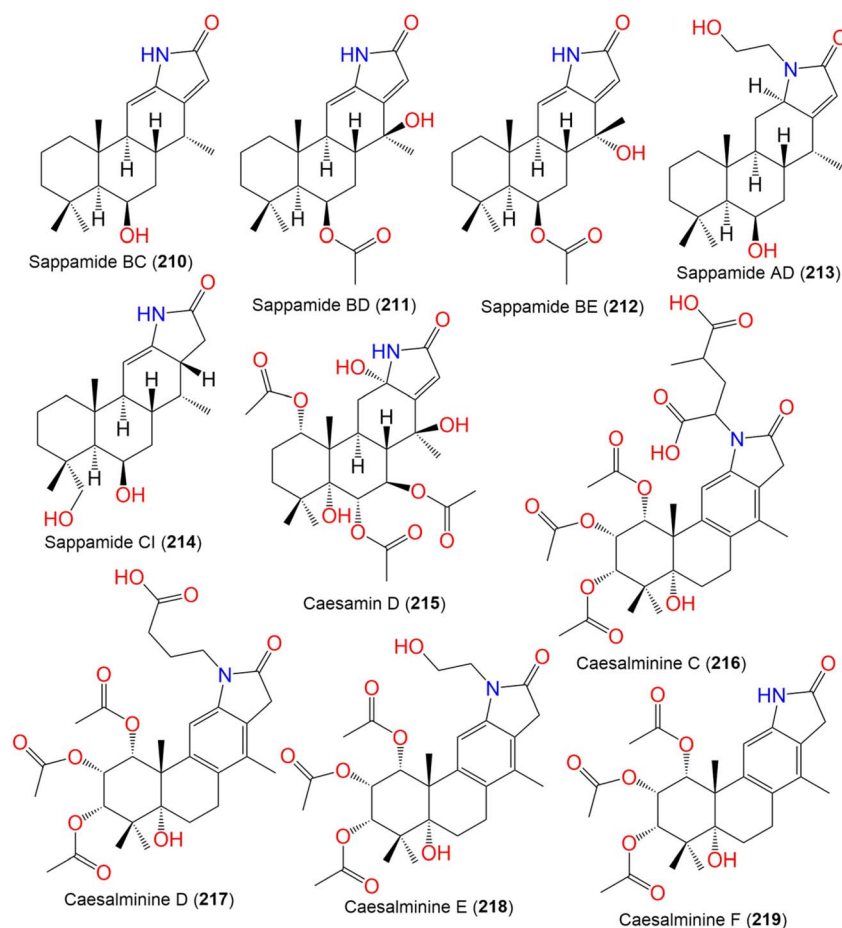


Fig. 23 Chemical structures of cassane diterpenoid alkaloids (210–219).

Compound **221** demonstrated substantial U87MG cell inhibitory capacity ( $IC_{50}$  10.5  $\mu$ M), while **224** had weak activity, suggesting C-12 methoxy boosted the activity.<sup>14</sup>

Compounds **225** and **226**, hexacyclic cassane alkaloids with a C-19 and C-20 amide bridge, were identified from *C. sappan* seeds (Table S8).<sup>35</sup> Compound **225** features a 6/6/6/5/6/5 skeleton with a 1,3-oxazolidine unit (ring F) incorporating the C-20 and N-atom of ring F, while **226** has 6/6/6/5/6/7 core skeleton with a 7-one-1,3-oxazepine ring F.<sup>35</sup> Their configurations are 4*R*/5*R*/8*S*/9*S*/10*S*/14*R*/20*R* and 4*R*/5*R*/8*S*/9*S*/10*S*/14*R*/20*R*, respectively based on ECD analyses. Compounds **225** and **226** demonstrated moderate cytotoxic effectiveness against MCF-7 cell line ( $IC_{50}$ s 27.23 and 29.67  $\mu$ M, respectively), compared to cisplatin ( $IC_{50}$  16.95  $\mu$ M).<sup>35</sup> Their biosynthesis starts with furanoditerpenoid (**A**) that is converted to **B** through oxidation reactions (Scheme 10). Then, amination and intramolecular cyclization of **B** yield a pentacyclic system with an amide bridge between C-19 and C-20. Finally, intramolecular cyclization of **E** produces **225** and **226**.<sup>35</sup>

A study by Wang *et al.* reported dimeric cassane diterpenoids, **227**, and **228** from *C. sappan* seeds EtOAc fraction. Compounds **227** and **228** are nitrogen-containing cassane diterpenoid dimer linked through an ether bond among C-20'/C-19. These compounds were assumed to be derived from methyl

20-hydroxyvinhaticoate through a series of chemical reactions, including oxidation, amination, reduction, and hydrogenation, as well as nucleophilic addition and intermolecular condensation (Scheme 11).

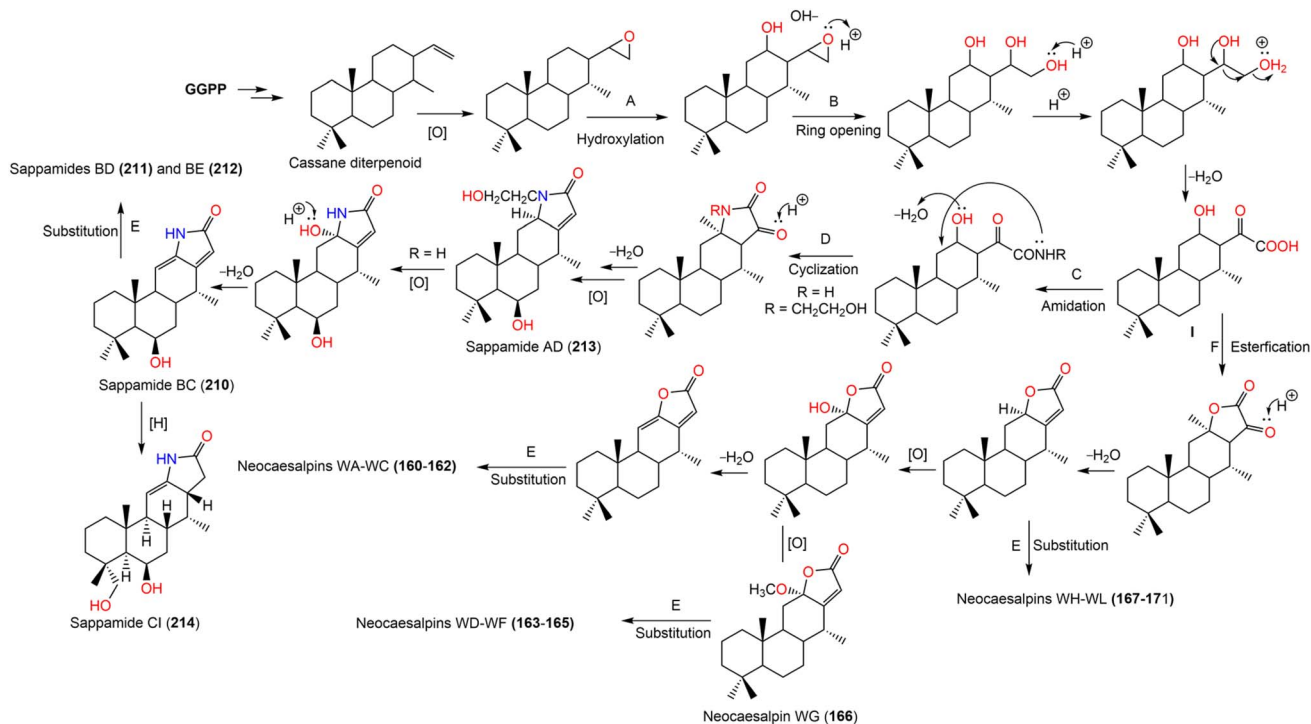
These compounds were assessed for their cytotoxic potential against HL-60, A-549, SMMC-7721, MCF-7, and SW480, and for inhibiting NO production induced by LPS in RAW 264.7. Compound **228** showed moderate cytotoxic effect against MCF-7 cell lines ( $IC_{50}$  29.98  $\mu$ M), compared to cisplatin ( $IC_{50}$  12.60  $\mu$ M), whereas **227** and **228** weakly prohibited NO production (% inhibition 36.01 and 32.93%, respectively; Conc. 50  $\mu$ M), compared to L-NMMA (%inhibition 54.36%) without toxicity against RAW 264.7 cells.<sup>52</sup>

#### 4.9. Cassaine diterpenoid ester amines and amides

From *Erythrophleum suaveolens* root bark MeOH extract, cassane diterpenoid amine; **229** and **231** were isolated. Their structures are related to 6*a*-hydroxy-*nor*-cassamine with a 3-hydroxy-3-methylbutanoyloxy at C-3. Compound **231** differs by having C-6 ketone and C-7 OH, instead of 6-OH and C-7 ketone in **229** (Fig. 25).<sup>10</sup>

Additionally, **233** and **234**, obtained from *Erythrophleum suaveolens* seeds extract, are cassane diterpenoid 3-





Scheme 9 Biosynthetic pathway of 160–171 and 210–214.<sup>17</sup> Adapted from ref. 17, with permission from the American Chemical Society. © 2021 American Chemical Society. License no. 6178300502704.

galactopyranosides with an ester amine side chain (cassamine or erythrophlamine analog), possessing 6-keto-7- $\beta$ -hydroxy and 6 $\alpha$ -hydroxy-7-keto unit, respectively.<sup>11</sup> Compound 233 ( $IC_{50}$ s 0.50, 6.26, and 7.30  $\mu$ M against A-549, MCF-7, and HCT-116, respectively) and 234 ( $IC_{50}$ s 4.92 and 6.75  $\mu$ M against A-549 and HCT-116, respectively) displayed cytotoxic efficacies, compared with doxorubicin ( $IC_{50}$ s 56.0, 90.0, and 120.0 nM).<sup>11</sup>

Kablan *et al.* separated 235 and 236 from *E. suaveolens* root barks, featuring N-methylaminoethanol residue amide bonded to the cassane diterpenoid core and galactose moiety attached to C-22 (Fig. 26). Compound 236 differs in having a 7-OH group instead of the carbonyl group in 235.<sup>11</sup>

#### 4.10. Other cassane diterpenoids

Compound 237 is a novel (5-hydroxy-7-methoxy-4-oxo-1-chroman-4-yl)-4-methoxy-*p*-benzoquinone-substituted cassane diterpenoid with a peroxide bridge between C-2 of breverin and C-11 of the diterpene part, which was obtained from Nigerian *Calliandra portoricensis* roots EtOAc extract (Table S9).<sup>53</sup> Compound 237 displayed potent anti *Trypanosoma* activity against *Trypanosoma brucei brucei* ( $EC_{50}$  0.69 and 0.33  $\mu$ g mL<sup>-1</sup> against a standard lab strain and multi-drug-resistant clone, respectively).<sup>53</sup> It caused irreversible apparent growth arrest and cell death after 2 h exposure in the resazurin-based assay. In addition, it exhibited moderate efficacy on *Leishmania mexicana* and *Trypanosoma congolense* with minimal toxicity on mammalian cells.<sup>53</sup> Additionally, compound 238, a new tricyclic cassane with  $\alpha$ ,  $\beta$ -unsaturated carbonyl moiety, was isolated from *Pterolobium macropterum* seeds.<sup>30</sup> This compound

inhibited LPS-simulated NO formation in BV-2 microglial cells ( $IC_{50}$  19.97  $\mu$ M).<sup>30</sup>

In the above-mentioned studies, cassane diterpenoids were assessed alongside standard reference drugs, which allows a rough comparison with currently used medicines. Overall, their activities are usually moderate and only occasionally comparable to the positive controls. For antibacterial assays, some cassane diterpenoids displayed activities comparable to gentamicin used in the same experiments, whereas other metabolites were clearly less active than the antibiotic controls. For enzyme-based assays, certain cassane derivatives exhibited  $\alpha$ -glucosidase and PTP1B inhibition that was similar to or slightly stronger than acarbose or suramin sodium, while many analogues were weak or inactive. In anti-inflammatory models, some derivatives suppressed LPS-induced NO production and iNOS expression at potencies comparable to reference inhibitors such as NG-monomethyl-L-arginine or quercetin, and a few metabolites slightly exceeded dexamethasone in this *in vitro* assay. In the other hand, in cytotoxicity studies most cassane diterpenoids displayed less potent activities than clinically used anticancer drugs such as doxorubicin, cisplatin or paclitaxel, indicating that cassane scaffolds may be viewed as early leads rather than direct alternatives. Similarly, in phytotoxic assays cassane diterpenoids were markedly less active than the commercial herbicide atrazine. Taken together, these comparisons indicated that cassane diterpenoids can reach or occasionally surpass the activity of reference drugs in certain *in vitro* models (*e.g.*, gentamicin, acarbose, suramin, quercetin,



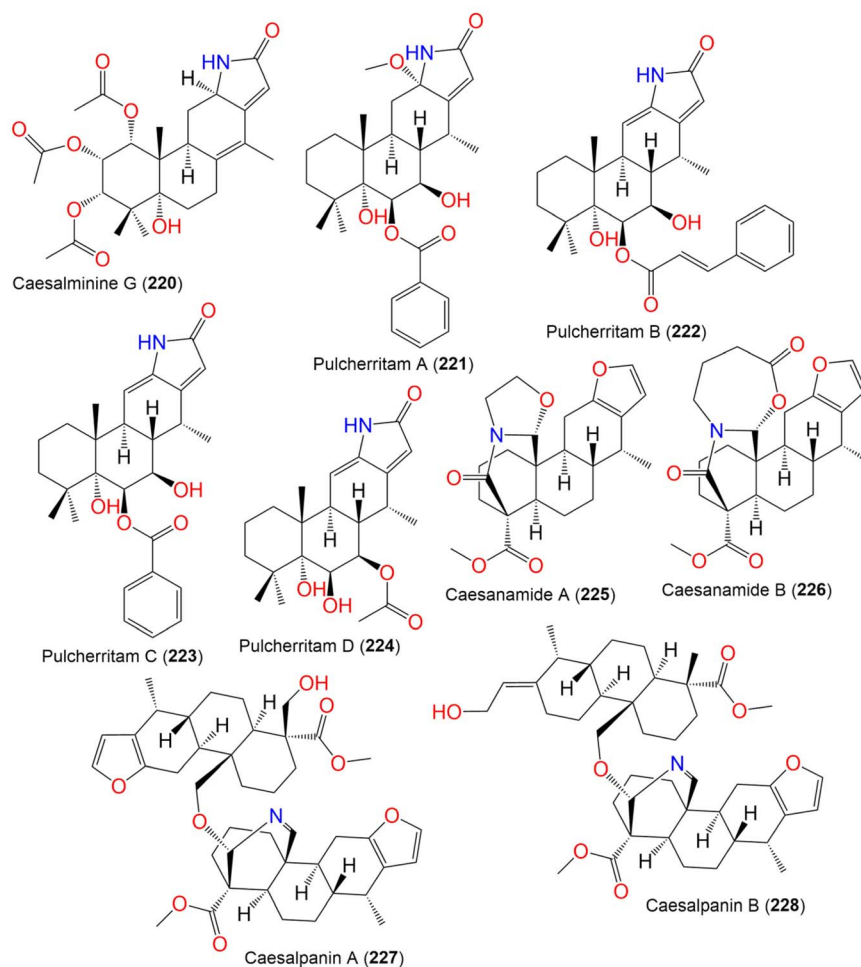
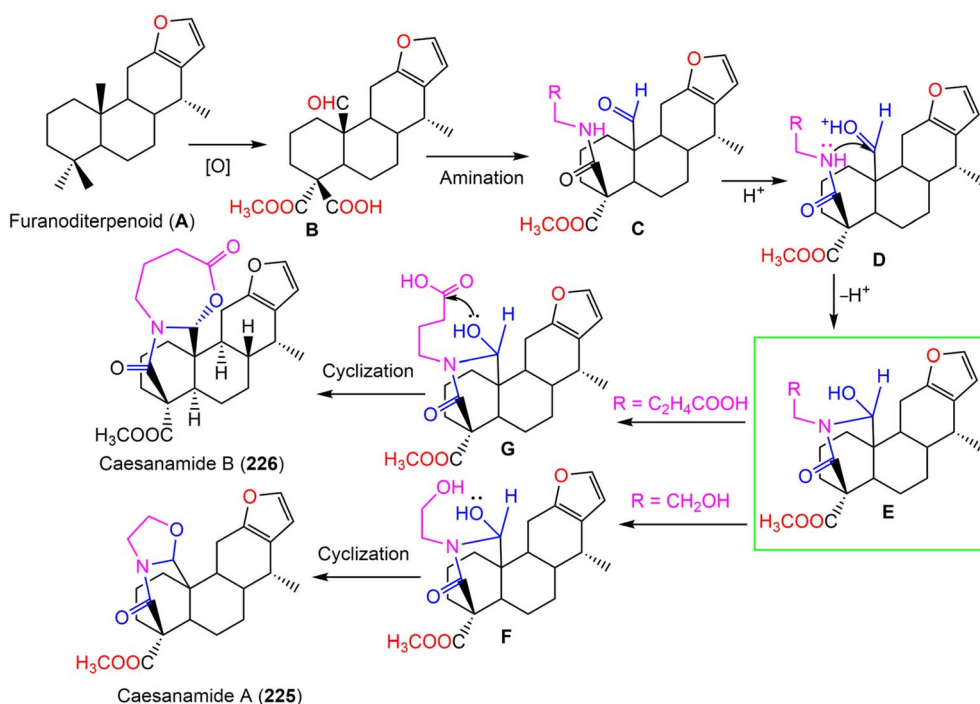
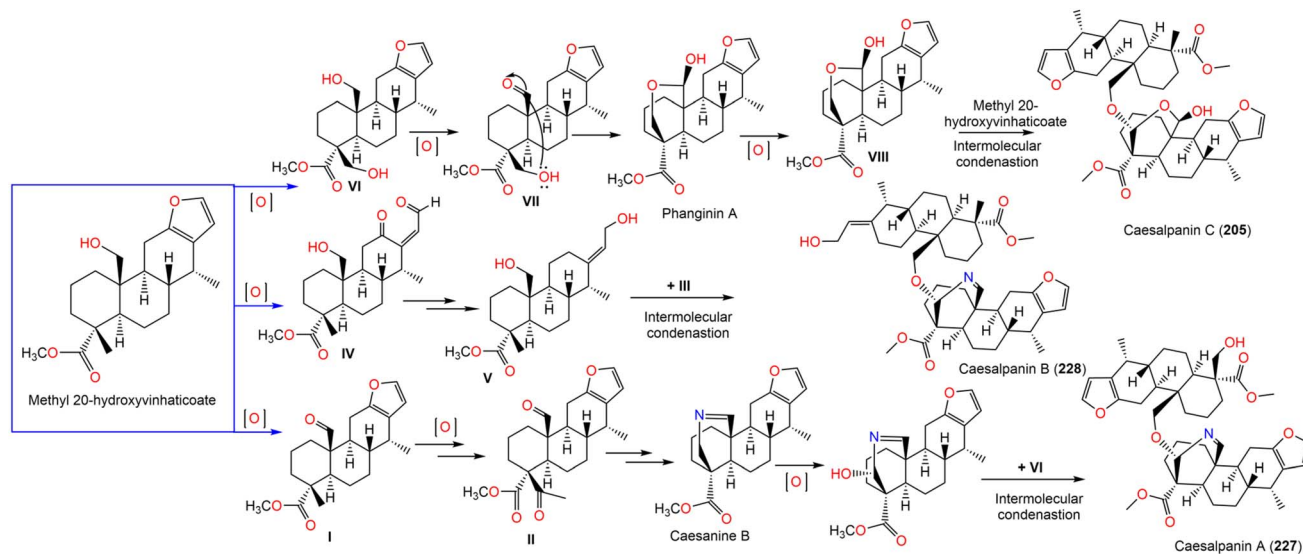


Fig. 24 Chemical structures of cassane diterpenoid alkaloids (220–228).



Scheme 10 Biosynthetic pathway of compounds 225 and 226.<sup>35</sup> Adapted from ref. 35, with permission from Elsevier. © 2022 Elsevier. License no. 6178030849466.





Scheme 11 Biosynthetic pathways of 205, 227, and 228.<sup>52</sup> Drawn by the authors based on ref. 52 (no third-party material reproduced). This article is an open access article distributed under the terms and conditions of the Creative Commons Attribution (CC BY) license.

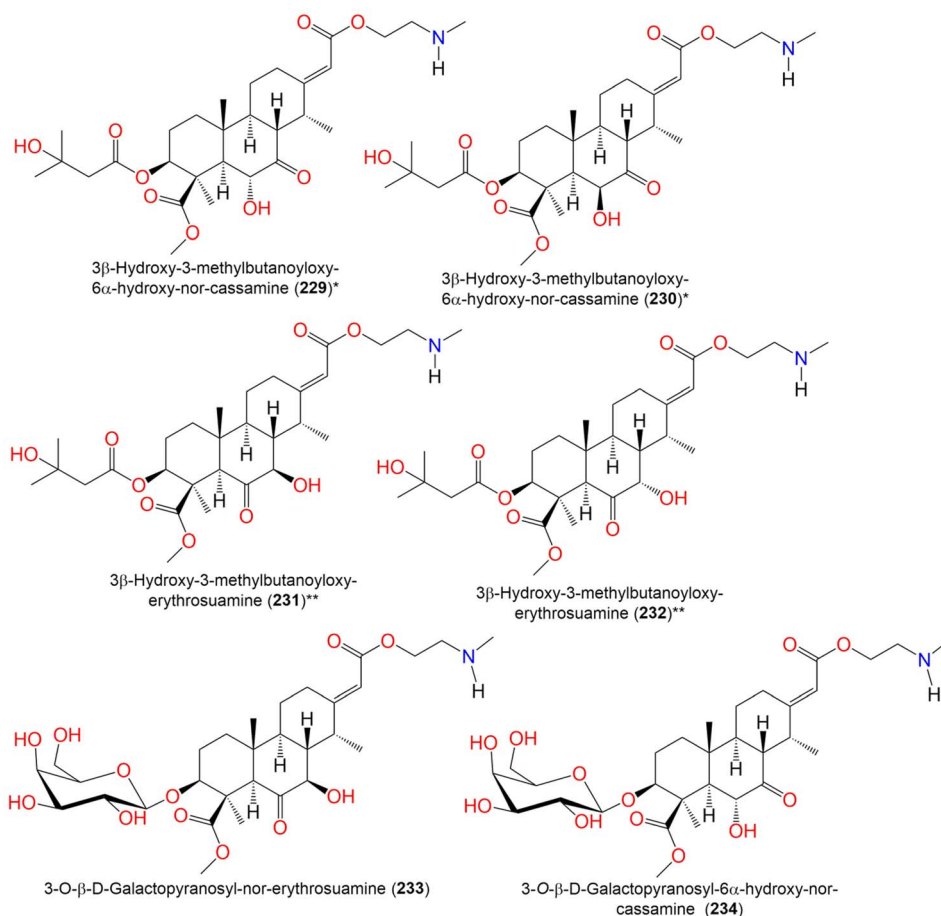


Fig. 25 Chemical structures of cassane diterpenoid ester amines (229–234). \*,\*\*Same name and different structures.



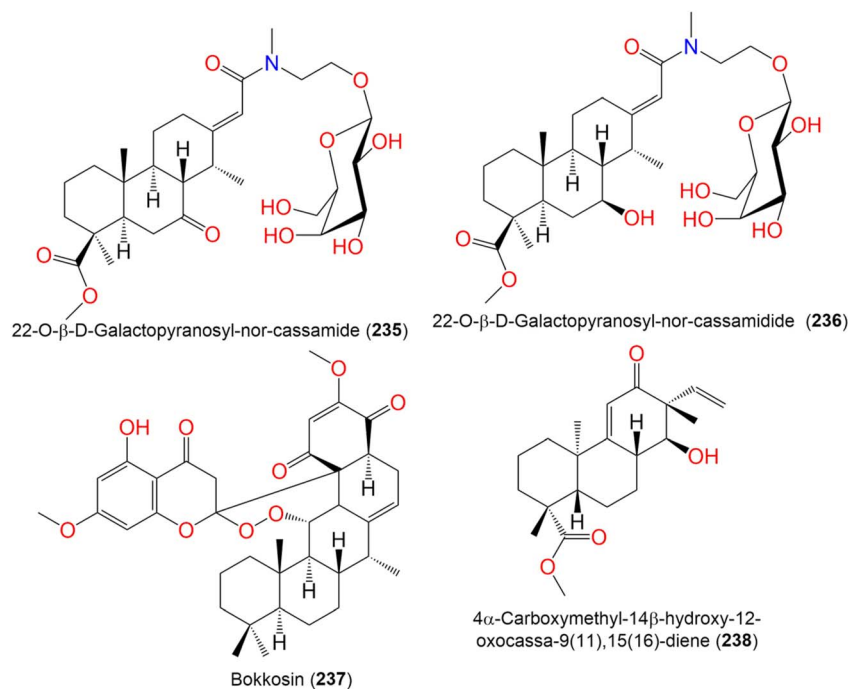


Fig. 26 Chemical structures of cassane diterpenoid amides (235 and 236) and others (237 and 238).

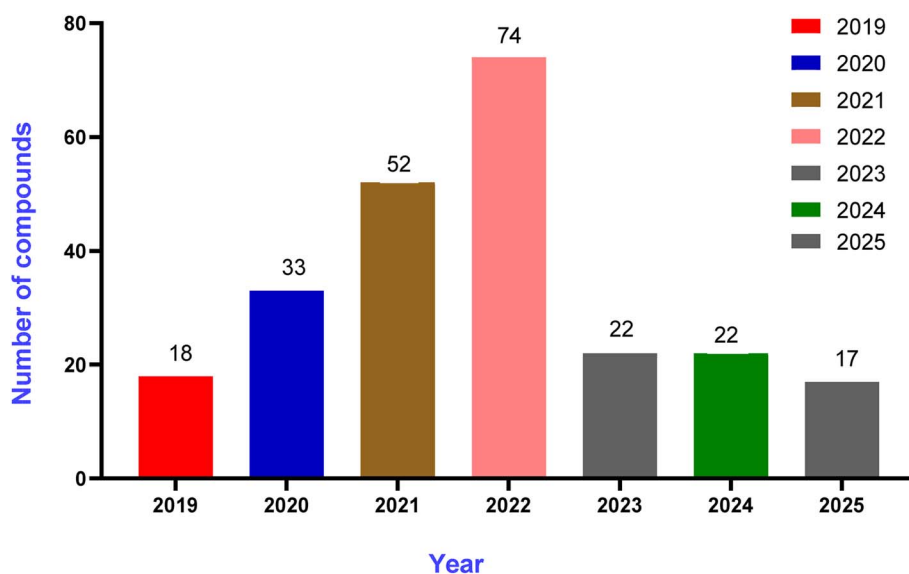


Fig. 27 Number of reported cassane diterpenoids in the period from 2019 to May 2025.

dexamethasone), but they generally did not outperform the potency of established therapeutic agents.

**4.10.1. Toxicological profile and safety considerations.** There is a lack of toxicological investigation for cassane diterpenoids themselves. The available data focused mainly on cassane-containing extracts. For example, acute oral toxicity studies on *C. pulcherrima* leaf, bark and flower extracts in mice and rats generally report no mortality at doses up to 2000–3000 mg kg<sup>-1</sup>, with calculated oral LD<sub>50</sub> of 5656.9 mg kg<sup>-1</sup> and only mild, dose-dependent signs such as drowsiness at the

highest doses, suggesting low acute toxicity.<sup>54,55</sup> These studies suggest that orally administered cassane-containing *Caesalpinia* extracts have relatively safety margins in acute models. Thus, there is a need for comprehensive vivo safety and pharmacokinetic studies on individual cassane diterpenoids.

## 5. Conclusion

Cassane diterpenoids are structurally diverse natural metabolites with broad pharmacological properties. In the current



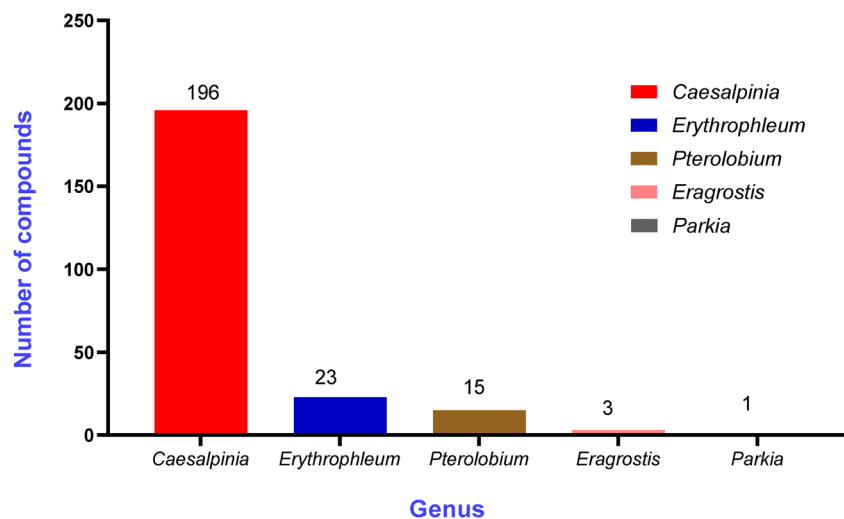


Fig. 28 Number of reported cassane diterpenoids from the *Fabaceae* family genera.

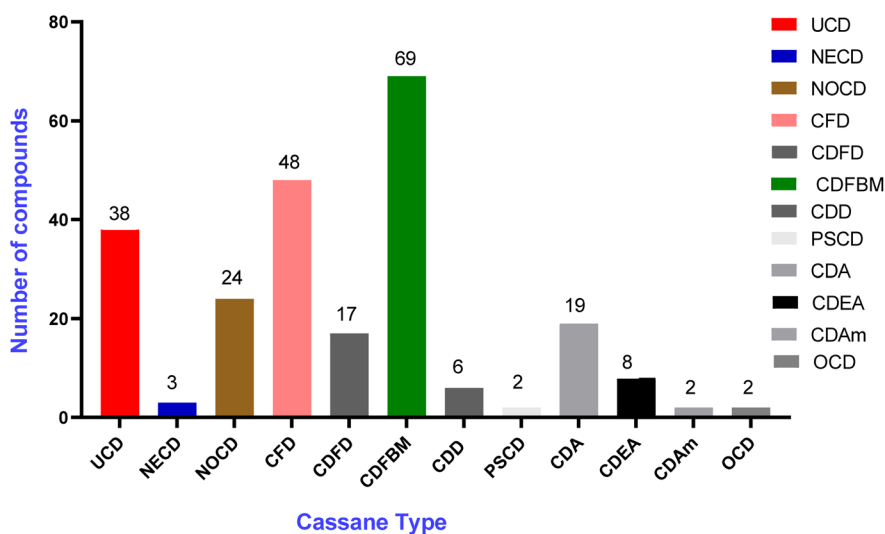


Fig. 29 Number of reported cassane diterpenoids from different classes.

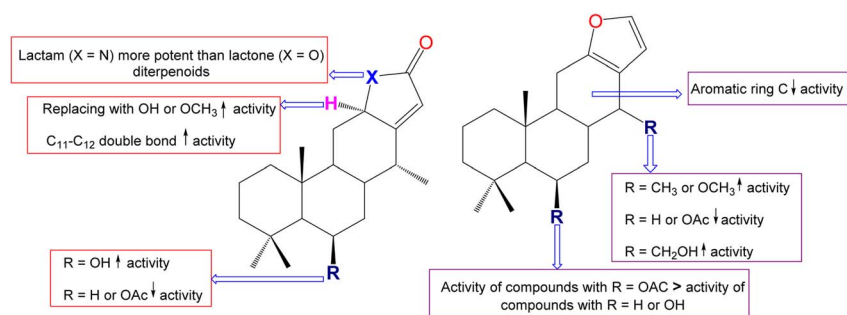


Fig. 30 Structure–activity relationship of the anti-inflammatory activity of butanolide and furan cassane diterpenoids.<sup>17,39</sup>

work, a total of 238 new cassane diterpenoids were reported in the period from 2019 to May 2025, with a notable rise in 2022 (74 compounds), followed by 2021 (52 compounds) (Fig. 27).

These compounds were identified from across the genera of family *Fabaceae*. Most of them were obtained from the *Caesalpinia* genus (196 compounds) (Fig. 28).



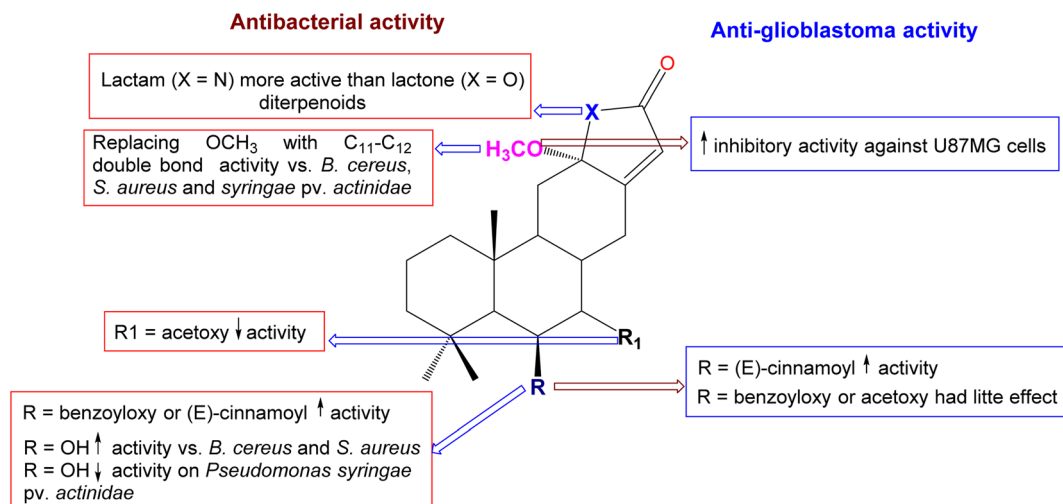


Fig. 31 Structure–activity relationship of the antibacterial and anti-glioblastoma activities.<sup>14</sup>

These diterpenoids were classified according to their skeleton into different subtypes, including cassane diterpenoids with fused butenolide moiety (69 compounds), furanoditerpenoids (48 compounds), usual cassane (38 compounds), and norcassane (24 compounds) (Fig. 29).

UCD, Usual cassane diterpenoids; NECD, Neocassane diterpenoids; NOCD, Norcassane diterpenoids; CFD, Cassane furanoditerpenoids; CDFD, Cassane dihydrofuran diterpenoids; CDFBM, Cassane diterpenoids with fused butenolide moiety; CCD, Cassane diterpenoid dimers; PSCD, Pentaspiro cassane diterpenoids; CDA, Cassane diterpenoid alkaloids; CDEA, Cassane diterpenoid ester amines; CDAm, Cassane diterpenoid amides; OCD, Other cassane diterpenoids.

Across literature, these metabolites have been assessed for different biological activities, with many demonstrating cytotoxic, antimicrobial, anti-inflammatory, anti-trypanosomal, antifungal, antiplasmodial, and  $\alpha$ -glucosidase and PTP1B inhibitory activities. For example, 12 and 67 exhibited anti-inflammatory effectiveness through suppressing NO production and iNOS activation, surpassing dexamethasone (reference drug) in certain assays, while 146, 225, and 226 showed significant cytotoxic activity, and 237 had potent anti-trypanosomal activity.

Additionally, some reports have outlined the structure–activity relationship of cassane diterpenoids, particularly for their anti-inflammatory, antibacterial, and anti-glioblastoma activities. It was found that these activities relied on their structural features and substitution patterns (Fig. 30 and 31).<sup>17,39</sup>

In butenolide and cassane furano-diterpenoids, the presence of a lactam moiety conferred higher potency than the lactone analogue. Introduction of hydroxyl or methoxy groups at C-12 and the presence of a C<sub>11</sub>-C<sub>12</sub> double bond further enhanced anti-inflammatory activity. For antibacterial and anti-glioblastoma activities (Fig. 31),<sup>14</sup> the replacement of lactone with lactam improved antibacterial activity, substituting C-12 methoxy with C<sub>11</sub>-C<sub>12</sub> double bond increased activity against *B. cereus*, *S. aureus*, and *Pseudomonas syringae* pv. *actinidiae*.

Additionally, (E)-cinnamoyl or benzyloxy groups at C-6 enhanced both antibacterial and anti-glioblastoma effects, while C-7 acetoxy substitution diminished activity.

Despite the growing number of new cassane diterpenoids, a limited number of them were biologically evaluated, mainly through *in vitro* assay. Therefore, more studies to elucidate their safety, *in vivo* efficacy, and mechanism of action, as well as semi-synthetic modification strategies and biosynthetic pathway elucidation, are needed.

## Author contributions

Sabrin R. M. Ibrahim conceived and designed the idea, analyzed the data, prepared figures and/or tables, wrote the draft of the paper, and approved the final draft. Hagar M. Mohamed analyzed the data, prepared figures and/or tables, authored or reviewed drafts of the paper, and approved the final draft. Samar S. A. Murshid analyzed the data, prepared figures and/or tables, authored or reviewed drafts of the paper, and approved the final draft. Asma Ahmad Nashawi analyzed the data, prepared figures and/or tables, authored or reviewed drafts of the paper, and approved the final draft. Gamal A. Mohamed conceived and designed the idea, analyzed the data, prepared figures and/or tables, wrote the draft of the paper, and approved the final draft.

## Conflicts of interest

The authors declare no competing interest.

## Data availability

No new data was generated or analyzed in this study. Data sharing is not applicable to this article as it is a review of previously published literature.

Supplementary information (SI) is available. See DOI: <https://doi.org/10.1039/d5ra07088k>.



## Acknowledgements

This Project was funded by the Deanship of Scientific Research (DSR) at King Abdulaziz University, Jeddah, Saudi Arabia under grant no. (DRP: 62-166-2025). The authors, therefore, acknowledge with thanks DSR for technical and financial support.

## References

- S. Khanam, P. Mishra, T. Faruqui, P. Alam, T. Albalawi, F. Siddiqui, Z. Rafi and S. Khan, *Front. Pharmacol*, 2025, **16**, 1587215, DOI: [10.3389/fphar.2025.1587215](https://doi.org/10.3389/fphar.2025.1587215).
- R. Maurya, M. Ravi, S. Singh and P. P. Yadav, *Fitoterapia*, 2012, **83**, 272–280, DOI: [10.1016/j.fitote.2011.12.007](https://doi.org/10.1016/j.fitote.2011.12.007).
- Y. Shen, W. Liang, Y. Shi, E. J. Kennelly and D. Zhao, *Nat. Prod. Rep.*, 2020, **37**, 763–796, DOI: [10.1039/D0NP00002G](https://doi.org/10.1039/D0NP00002G).
- J. Zhang, W. M. Abdel-Mageed, M. Liu, P. Huang, W. He, L. Li, F. Song, H. Dai, X. Liu, J. Liang and L. Zhang, *Org. Lett.*, 2013, **15**, 4726–4729, DOI: [10.1021/ol402058z](https://doi.org/10.1021/ol402058z).
- A. Raksat, T. Aree and K. Pudhom, *J. Nat. Prod.*, 2020, **83**, 2241–2245, DOI: [10.1021/acs.jnatprod.0c00354](https://doi.org/10.1021/acs.jnatprod.0c00354).
- S. Cheenpracha, R. Chokchaisiri, L. Ganranoo, S. Bureekaew, T. Limtharakul and S. Laphookhieo, *Beilstein J. Org. Chem.*, 2023, **19**, 658–665, DOI: [10.3762/bjoc.19.47](https://doi.org/10.3762/bjoc.19.47).
- W. Jing, X. Zhang, H. Zhou, Y. Wang, M. Yang, L. Long and H. Gao, *Fitoterapia*, 2019, **134**, 226–249, DOI: [10.1016/j.fitote.2019.02.023](https://doi.org/10.1016/j.fitote.2019.02.023).
- A. Favaretto, C. L. Cantrell, F. R. Fronczek, S. O. Duke, D. E. Wedge, A. Ali and S. M. Scheffer-Basso, *J. Agric. Food Chem.*, 2019, **67**, 1973–1981, DOI: [10.1021/acs.jafc.8b06832](https://doi.org/10.1021/acs.jafc.8b06832).
- D. S. Wang, Y. Shen, L. F. Ding, R. C. Yan, M. Hu, W. C. Tu, L. D. Song, S. Huang and X. D. Wu, Cassane diterpenoids with hepatic gluconeogenesis inhibitory activity from the seeds of *Caesalpinia decapetala* (Roth) Alston, *Phytochemistry*, 2025, **240**, 114628, DOI: [10.1016/j.phytochem.2025.114628IF](https://doi.org/10.1016/j.phytochem.2025.114628IF).
- J. D. Konan, B. K. Attioua, C. L. A. Kablan, F. A. Kabran, P. A. Koffi, S. A. Any-Grah, S. Drissa, B. Seon-Meniél, K. LeBlanc, J. Jullian and M. A. Beniddir, *Phytochem. Lett.*, 2019, **31**, 166–169, DOI: [10.1016/j.phytol.2019.04.001](https://doi.org/10.1016/j.phytol.2019.04.001).
- A. C. L. Kablan, J. D. Konan, G. Komlaga, F. A. Kabran, B. Daouda, A. D. N'Tamon, T. Kouamé, A. Jagora, K. Leblanc and B. Seon-Méniél, *Fitoterapia*, 2020, **146**, 104700.
- C. Huang, Y. Xu, J. Chen, Z. Feng, Q. Zhang and L. Lin, *Phytochem. Lett.*, 2021, **43**, 163–168, DOI: [10.1016/j.phytol.2021.03.018](https://doi.org/10.1016/j.phytol.2021.03.018).
- M. F. Chen, Y. Zhang, P. Zhang and R. Shu, *J. Asian Nat. Prod. Res.*, 2022, **24**, 1134–1140, DOI: [10.1080/10286020.2022.2026933](https://doi.org/10.1080/10286020.2022.2026933).
- X. Chen, W. Lu, Z. Zhang, J. Zhang, T. M. L. Tuong, L. Liu, Y. H. Kim, C. Li and J. Gao, *Phytochemistry*, 2022, **196**, 113082, DOI: [10.1016/j.phytochem.2021.113082](https://doi.org/10.1016/j.phytochem.2021.113082).
- X. Chen, W. Lu, Z. Zhang, P. Wang, X. Zhang, C. Xiao, Q. Zhang, J. Gao and C. Li, *Pest Manag. Sci.*, 2023, **79**, 2539–2555, DOI: [10.1002/ps.7430](https://doi.org/10.1002/ps.7430).
- M. Wang, T. Zhu, S. Yu, T. Liu, B. Zhou and H. Gao, *Nat. Prod. Res.*, 2022, **36**, 5032–5038.
- M. Wang, S. Yu, S. Qi, B. Zhang, K. Song, T. Liu and H. Gao, *J. Nat. Prod.*, 2021, **84**, 2175–2188, DOI: [10.1021/acs.jnatprod.1c00233](https://doi.org/10.1021/acs.jnatprod.1c00233).
- P. Li, B. Zhang, Z. Zhu, W. Jing, M. Wang and H. Gao, *Phytochem. Lett.*, 2022, **47**, 115–119, DOI: [10.1016/j.phytol.2021.12.004](https://doi.org/10.1016/j.phytol.2021.12.004).
- A. C. da Silva, T. Tizziani, T. L. Lubschinski, P. Fragoso, B. K. Beck, B. G. L. Soares, O. L. Guterres Fernandes, A. J. Bortoluzzi, E. M. Dalmarco and L. P. Sandjo, *Fitoterapia*, 2025, **184**, 106638, DOI: [10.1016/j.fitote.2025.106638](https://doi.org/10.1016/j.fitote.2025.106638).
- W. Tu, L. Ding, L. Peng, L. Song, X. Wu and Q. Zhao, *Phytochemistry*, 2022, **193**, 112973, DOI: [10.1016/j.phytochem.2021.112973](https://doi.org/10.1016/j.phytochem.2021.112973).
- J. Dibi Konan, F. Aka Kabran, B. Koffi Attioua, L. C. Ahmont Kablan, S. Any-Grah Aka, A. Angely Koffi, A. Ouoyogodé Akoubet, E. N'ngang Otogo, B. Seon-Meniél, K. L. Blanc, J. Jullian, D. Sissouma, M. A. Beniddir and P. Champy, *Nat. Prod. Res.*, 2021, **35**, 1364–1371, DOI: [10.1080/14786419.2019.1650354](https://doi.org/10.1080/14786419.2019.1650354).
- Y. Xu, W. Shi, L. Feng, J. Cao, Z. Feng, Q. Zhang, J. Lu, Y. Ye and L. Lin, *Nat. Prod. Res.*, 2022, **36**, 932–941, DOI: [10.1080/14786419.2020.1853729](https://doi.org/10.1080/14786419.2020.1853729).
- M. Wang, X. Zhang, M. Qi, D. Guo, Y. Wang and H. Gao, *Fitoterapia*, 2021, **153**, 104978, DOI: [10.1016/j.fitote.2021.104978](https://doi.org/10.1016/j.fitote.2021.104978).
- W. Lu, J. Chen, Y. Shi, M. Chen, P. Wang, X. Zhang, C. Xiao, D. Li, C. Cao, C. Li and J. Gao, *J. Ethnopharmacol.*, 2023, **315**, 116653, DOI: [10.1016/j.jep.2023.116653](https://doi.org/10.1016/j.jep.2023.116653).
- F. R. E. Essoung, B. M. Mba'ning, A. T. Tcho, S. C. Chhabra, S. A. Mohamed, B. N. Lenta, S. A. Ngouela, E. Tsamo, A. Hassanali and R. J. Cox, *Nat. Prod. Res.*, 2021, **35**, 5681–5691, DOI: [10.1080/14786419.2020.1825424](https://doi.org/10.1080/14786419.2020.1825424).
- M. B. Bitchi, A. A. Magid, P. A. Yao-Kouassi, F. A. Kabran, D. Harakat, A. Martinez, H. Morjani, F. Z. Tonzibo and L. Voutquenne-Nazabadioko, *Fitoterapia*, 2019, **137**, 104264, DOI: [10.1016/j.fitote.2019.104264](https://doi.org/10.1016/j.fitote.2019.104264).
- T. Grkovic, J. R. Evans, R. K. Akee, L. Guo, M. Davis, J. Jato, P. G. Grothaus, M. Ahalt-Gottholm, M. Hollingshead, J. M. Collins, D. J. Newman and B. R. O'Keefe, *Bioorg. Med. Chem. Lett.*, 2019, **29**, 134–137, DOI: [10.1016/j.bmcl.2018.12.019](https://doi.org/10.1016/j.bmcl.2018.12.019).
- L. Li, L. Chen, Y. Li, S. Sun, S. Ma, Y. Li and J. Qu, *Phytochemistry*, 2020, **174**, 112343, DOI: [10.1016/j.phytochem.2020.112343](https://doi.org/10.1016/j.phytochem.2020.112343).
- X. Zhang, Y. Yin, Y. Zhou, T. Zhu, M. Wang and H. Gao, *Chin. J. Chem.*, 2022, **40**, 617–627.
- Y. Lan, W. Gu, M. Yang and P. Zhang, *Phytochem. Lett.*, 2024, **62**, 44–48, DOI: [10.1016/j.phytol.2024.06.008](https://doi.org/10.1016/j.phytol.2024.06.008).
- Z. Zhang, P. Wang, M. Chen, L. Xie, X. Zhang, Y. Shi, W. Lu, Q. Zhang and C. Li, *Int. J. Mol. Sci.*, 2023, **24**, 4917, DOI: [10.3390/ijms24054917](https://doi.org/10.3390/ijms24054917).
- L. Lian, Y. Yang, D. Guo, Y. Yan, H. Gao, X. Li and M. Wang, *J. Asian Nat. Prod. Res.*, 2022, **24**, 979–986, DOI: [10.1080/10286020.2021.2004130](https://doi.org/10.1080/10286020.2021.2004130).



- 33 R. V. K. Tchibou, P. Eckhardt, B. M. Kemkuignou, R. Tchounguem, R. T. Fouedjou, B. K. Ponou, J. P. Dzoyem, R. B. Teponno, L. Barboni and T. Opatz, *Phytochem. Lett.*, 2022, **48**, 62–67, DOI: [10.1016/j.phytol.2022.02.001](https://doi.org/10.1016/j.phytol.2022.02.001).
- 34 J. Su, D. Wang, G. Hu, Y. Liu, M. Hu, Y. Chen, Q. Wang, R. Yan, Y. Wu and Y. Li, *Phytochemistry*, 2024, **222**, 114105, DOI: [10.1016/j.phytochem.2024.114105](https://doi.org/10.1016/j.phytochem.2024.114105).
- 35 Y. Jin, M. Wang, Y. Yan, X. Zhang, X. Li and H. Gao, *Phytochemistry*, 2022, **197**, 113111, DOI: [10.1016/j.phytochem.2022.113111](https://doi.org/10.1016/j.phytochem.2022.113111).
- 36 Q. Ruan, X. Zhou, S. Jiang, B. Yang, J. Jin, H. Cui and Z. Zhao, *Fitoterapia*, 2019, **134**, 50–57, DOI: [10.1016/j.fitote.2019.02.004](https://doi.org/10.1016/j.fitote.2019.02.004).
- 37 T. Liu, M. Wang, S. Qi, X. Shen, Y. Wang, W. Jing, Y. Yang, X. Li and H. Gao, *Bioorg. Chem.*, 2020, **96**, 103573.
- 38 M. Wang, J. Zhou, X. Zhang, J. Ma, Y. Wu, Y. Zhao and H. Gao, *Bioorg. Chem.*, 2025, **158**, 108333, DOI: [10.1016/j.bioorg.2025.108333](https://doi.org/10.1016/j.bioorg.2025.108333).
- 39 M. Wang, Y. Yang, Y. Yin, K. Song, L. Long, X. Li, B. Zhou and H. Gao, *Chin. J. Chem.*, 2021, **39**, 1625–1634, DOI: [10.1002/cjoc.202000683](https://doi.org/10.1002/cjoc.202000683).
- 40 J. Cao, Y. Xu, R. Lou, W. Shi, J. Chen, L. Gan, J. Lu and L. Lin, *Chem. Biodivers.*, 2021, **18**, e2100309, DOI: [10.1002/cbdv.202100309](https://doi.org/10.1002/cbdv.202100309).
- 41 J. Yuanting, H. Ruikang, L. Yang and L. Hanqiao, *Nat. Prod. Res.*, 2022, **36**, 2078–2084, DOI: [10.1080/14786419.2020.1849196](https://doi.org/10.1080/14786419.2020.1849196).
- 42 W. Tu, L. Ding, L. Song, Y. Li, R. Yan, Y. Wu, W. Feng and X. Wu, *Phytochemistry*, 2024, **225**, 114189, DOI: [10.1016/j.phytochem.2024.114189](https://doi.org/10.1016/j.phytochem.2024.114189).
- 43 A. Raksat, S. Choodej, T. Aree, S. N. Ebrahimi and K. Pudhom, *Phytochemistry*, 2022, **196**, 113074, DOI: [10.1016/j.phytochem.2021.113074](https://doi.org/10.1016/j.phytochem.2021.113074).
- 44 R. Lou, F. Xu, Y. Xu, J. Chen, Z. Feng, L. Gan and L. Lin, *Bioorg. Chem.*, 2021, **117**, 105426, DOI: [10.1016/j.bioorg.2021.105426](https://doi.org/10.1016/j.bioorg.2021.105426).
- 45 C. Li, J. Zhang, T. M. L. Tuong, Y. Liu, X. N. Hoang and J. Gao, *J. Agric. Food Chem.*, 2020, **68**, 4227–4236, DOI: [10.1021/acs.jafc.0c00853](https://doi.org/10.1021/acs.jafc.0c00853).
- 46 Y. Jin, Z. Tong, H. Gao and Z. Wu, *Chem. Biodivers.*, 2023, **20**, e202300211, DOI: [10.1002/cbdv.202300211](https://doi.org/10.1002/cbdv.202300211).
- 47 X. Yun, X. Chen, J. Wang, W. Lu, Z. Zhang, Y. H. Kim, S. Zong, C. Li and J. Gao, *Nat. Prod. Res.*, 2022, **36**, 4630–4638, DOI: [10.1080/14786419.2021.2007096](https://doi.org/10.1080/14786419.2021.2007096).
- 48 V. H. Son, N. T. T. Hau, N. T. M. Thu, T. T. V. Hoa, N. H. Hoang, N. T. Cuc, B. H. Tai, D. T. Thao, P. Van Kiem and N. X. Nhiem, *Phytochem. Lett.*, 2022, **47**, 93–96, DOI: [10.1016/j.phytol.2021.11.011](https://doi.org/10.1016/j.phytol.2021.11.011).
- 49 H. Xie, T. Long, Y. Gao, D. Huang and L. Wang, *Fitoterapia*, 2025, **183**, 106500, DOI: [10.1016/j.fitote.2025.106500](https://doi.org/10.1016/j.fitote.2025.106500).
- 50 Y. Xu, T. Zhang, L. Feng, Z. Feng, Q. Zhang, Y. Ye, L. Gan and L. Lin, *Chin. Chem. Lett.*, 2021, **32**, 1475–1479, DOI: [10.1016/j.cclet.2020.09.048](https://doi.org/10.1016/j.cclet.2020.09.048).
- 51 S. Yan, S. Huang, J. Xing, Y. Cai, Y. Ruan and P. Zhang, *Fitoterapia*, 2024, **173**, 105834, DOI: [10.1016/j.fitote.2024.105834](https://doi.org/10.1016/j.fitote.2024.105834).
- 52 D. Wang, W. Nie, T. Jiang, L. Ding, L. Song, X. Wu and Q. Zhao, *Chem. Biodivers.*, 2020, **17**, e2000103, DOI: [10.1002/cbdv.202000103](https://doi.org/10.1002/cbdv.202000103).
- 53 J. B. Nvau, S. Alenezi, M. A. Ungogo, I. A. Alfayez, M. J. Natto, A. I. Gray, V. A. Ferro, D. G. Watson, H. P. De Koning and J. O. Igoli, *Front. Chem.*, 2020, **8**, 574103, DOI: [10.3389/fchem.2020.574103](https://doi.org/10.3389/fchem.2020.574103).
- 54 O. K. Ogbeide, V. O. Dickson, R. D. Jebba, D. A. Owhiroro, M. O. Olaoluwa, V. O. Imieje, O. Erharuyi, B. J. Owolabi, P. Fasinu and A. Falodun, *Trop. J. Nat. Prod. Res.*, 2018, **2**, 179–184, DOI: [10.26538/tjnpr/v2i4.5](https://doi.org/10.26538/tjnpr/v2i4.5).
- 55 J. O. Uadia, N. Chigozie, V. I. Ndubisi and O. K. Ogbeide, *Walisongo J. Chem.*, 2023, **6**, 194–207, DOI: [10.21580/wjc.v6i2.18175](https://doi.org/10.21580/wjc.v6i2.18175).

